THE JOURNAL OF BIOLOGICAL CHEMISTRY VOL. 289, NO. 24, pp. 16773–16789, June 13, 2014

Lipocalin-2 Protein Deficiency Ameliorates Experimental Autoimmune Encephalomyelitis

*THE PATHOGENIC ROLE OF LIPOCALIN-2 IN THE CENTRAL NERVOUS SYSTEM AND PERIPHERAL LYMPHOID TISSUES**

Received for publication, December 14, 2013, and in revised form, April 25, 2014 Published, JBC Papers in Press, May 7, 2014, DOI 10.1074/jbc.M113.542282

Youngpyo Nam[‡], Jong-Heon Kim[‡], Minchul Seo[‡1], Jae-Hong Kim[‡], Myungwon Jin[‡], Sangmin Jeon[‡2], Jung-wan Seo[‡3], Won-Ha Lee[§], So Jin Bing[¶], Youngheun Jee[¶], Won Kee Lee[‖], Dong Ho Park[**], Hyun Kook[‡‡], and Kyoungho Suk[‡4]

From the [‡]Department of Pharmacology, Brain Science and Engineering Institute, and Department of Biomedical Sciences, BK21 Plus KNU Biomedical Convergence Program, Kyungpook National University School of Medicine, Daegu 700-422, Korea, [§]School of Life Sciences and Biotechnology, Kyungpook National University, Daegu 702-701, Korea, [¶]College of Veterinary Medicine and Applied Radiological Institute, Jeju National University, Jeju 690-756, Korea, [‖]Center of Biostatistics, Kyungpook National University School of Medicine, Daegu 700-422, Korea, [**]Department of Ophthalmology, Kyungpook National University School of Medicine, Daegu 700-422, Korea, and [‡‡]Department of Pharmacology, Chonnam National University Medical School, Gwangju 501-746, Korea

Background: The role of LCN2 in EAE is not clear.
Results: LCN2 expression increased in EAE. *Lcn2* deficiency attenuated EAE symptoms and pathology. LCN2 enhanced glial expression of inflammatory mediators and peripheral encephalitogenic T cell activation *in vitro* and *in vivo*.
Conclusion: Both central and peripheral LCN2 contributed to EAE development.
Significance: LCN2 can be targeted for treatment of multiple sclerosis.

Lipocalin-2 (LCN2) plays an important role in cellular processes as diverse as cell growth, migration/invasion, differentiation, and death/survival. Furthermore, recent studies indicate that LCN2 expression and secretion by glial cells are induced by inflammatory stimuli in the central nervous system. The present study was undertaken to examine the regulation of LCN2 expression in experimental autoimmune encephalomyelitis (EAE) and to determine the role of LCN2 in the disease process. LCN2 expression was found to be strongly increased in spinal cord and secondary lymphoid tissues after EAE induction. In spinal cords astrocytes and microglia were the major cell types expressing LCN2 and its receptor 24p3R, respectively, whereas in spleens, LCN2 and 24p3R were highly expressed in neutrophils and dendritic cells, respectively. Furthermore, disease severity, inflammatory infiltration, demyelination, glial activation, the expression of inflammatory mediators, and the proliferation of MOG-specific T cells were significantly attenuated in *Lcn2*-deficient mice as compared with wild-type animals. Myelin oligodendrocyte glycoprotein-specific T cells in culture exhibited an increased expression of *Il17a*, *Ifng*, *Rorc*, and *Tbet* after treatment with recombinant LCN2 protein. Moreover, LCN2-treated glial cells expressed higher levels of proinflammatory cytokines, chemokines, and MMP-9. Adoptive transfer and recombinant LCN2 protein injection experiments suggested that LCN2 expression in spinal cord and peripheral immune organs contributes to EAE development. Taken together, these results imply LCN2 is a critical mediator of autoimmune inflammation and disease development in EAE and suggest that LCN2 be regarded a potential therapeutic target in multiple sclerosis.

Multiple sclerosis (MS)[5] is a chronic inflammatory disease of the central nervous system (CNS) characterized by immune cell infiltration and demyelination of the brain and spinal cord (1–3). In MS, inflammatory reactions involve complex interactions between infiltrating immune cells and resident CNS cells that lead to inflammatory lesion formation, demyelination, oligodendrocyte, and axonal damage (4, 5). Experimental autoimmune encephalomyelitis (EAE) is an animal model widely used to study neuroimmunologic responses in MS. The key players in MS, which include T cells (6–8), B cells (9–11), mast cells (12, 13), macrophages (14), CNS resident glial cells (15, 16), adhesion molecules (17, 18), cytokines, and chemokines (19,

* This work was supported by National Research Foundation of Korea Grant 2008-0062282 funded by the Korean government (MSIP) and by Korean Health Technology R&D Project, Korean Ministry of Health and Welfare Grant A111345.

[1] Present address: Dongguk University College of Medicine, 123 Dongdae-ro, Gyeongju, Gyeongsangbuk-do 780-714, Korea.
[2] Present address: Dept. of Neurosurgery, Biological Chemistry, and Neuroscience, Neurosurgery Pain Research Institute, Johns Hopkins School of Medicine, Baltimore, MD 21205.
[3] Present address: Daesang Corp. Customer Support Division, Food Safety Center 697 Jungbu-daero, Majang-myeon, Icheon, Gyeonggi-do 467-813, Korea.
[4] To whom correspondence should be addressed: Department of Pharmacology, Kyungpook National University School of Medicine, 101 Dong-In, Joong-gu, Daegu, 700-422, Republic of Korea. Tel.: 82-53-420-4835; Fax: 82-53-256-1566; E-mail: ksuk@knu.ac.kr.

[5] The abbreviations used are: MS, multiple sclerosis; EAE, experimental autoimmune encephalomyelitis; GFAP, glial fibrillary acidic protein; Iba-1, ionized calcium binding adapter molecule 1; Ly6G, lymphocyte antigen 6G; LCN2, lipocalin-2; MOG, myelin oligodendrocyte glycoprotein; MMP, matrix metalloproteinase; *Rorc*, RAR-related orphan receptor C; *Tbet*, T-box transcription factor.

20), have been shown to mediate disease development and progress in EAE.

Lipocalin 2 (LCN2), also termed 24p3 (21), uterocalin (22), and neutrophil gelatinase-associated lipocalin (NGAL) (23), is a member of the lipocalin family, a group of small extracellular proteins with great functional diversity (24–26). LCN2 has been shown to regulate diverse cellular processes, such as cell growth, migration/invasion, differentiation, and death/survival as well as iron delivery (22, 27–30). LCN2 expression is induced under many inflammatory conditions, such as inflammatory bowel disease (31), psoriasis (32), rheumatoid arthritis (33), and systemic lupus erythematosus (34). Furthermore, recent studies have provided evidence that LCN2 secretion can be induced by IL-17 (35, 36), a Th17 cell-derived cytokine that contributes to the pathogenesis of many autoimmune and inflammatory diseases. LCN2 has also been implicated in CNS inflammation, mild cognitive impairment (37), Alzheimer disease (38), amyotrophic lateral sclerosis (39), and frontotemporal lobar degeneration (40). In a previous study we reported that LCN2 is secreted by microglia and astrocytes in culture (41) and that LCN2 induces chemokine production (42) and microglial M1 polarization in the CNS (43). Other laboratories have reported that LCN2 expression increases in the CNS after systemic LPS injection (44) or by kainate-induced excitotoxicity (45). In addition, LCN2 was up-regulated in astrocytes, neurons, and neutrophils after spinal cord injury, and *Lcn2*-deficient mice showed reduced leukocyte infiltration and levels of proinflammatory mediators, such as MCP-1, TNF-α, IL-1β, IL-6, and inducible nitric-oxide synthase, after spinal cord injury (46), suggesting that LCN2 is likely to play an important role in CNS inflammation and related diseases. LCN2 is recognized by cell surface receptor 24p3R, a brain-type organic cation transporter (BOCT) (28). The expression of 24p3R has been detected in glia and neurons in the CNS, and recent studies have shown that LCN2 regulates neuronal migration, morphology (47), and excitability (48). These previous reports suggest that LCN2 has pleiotropic roles in different aspects of CNS physiology and pathology. In particular, the reported associations between LCN2 and IL-17 and chemokine expression strongly suggest its involvement in EAE, MS, and other inflammatory diseases of the CNS.

In this study we investigated the involvement of LCN2 in the pathogenesis of EAE. LCN2 expression was increased in spinal cord, lymph nodes, and spleen during EAE. *Lcn2* deficiency significantly attenuated disease severity, inflammatory infiltration, demyelination, and the expression of inflammatory cytokines and chemokines. Furthermore, recombinant LCN2 protein enhanced the activation of encephalitogenic T cells and CNS-resident glial cells, and adoptive transfer and LCN2 protein injection experiments showed that LCN2 expression in the CNS and peripheral lymphoid tissues is critically involved in the development of EAE.

EXPERIMENTAL PROCEDURES

Animals—Wild-type (WT) and *Lcn2* knock-out (KO) C57BL/6 mice were obtained from Samtaco (Osan, Korea) and Dr. Shizuo Akira (Osaka University, Japan), respectively. *Lcn2* KO mice were back-crossed for 8–10 generations in a C57BL/6 background to generate homozygous and heterozygous animals, as described previously (49, 50). The absence of *Lcn2* in *Lcn2*-deficient mice was confirmed by PCR of genomic DNA. Animals used in the present study were acquired and cared for in accordance with the "Guide for the Care and Use of Laboratory Animals" published by the National Institutes of Health.

EAE Induction—Mice (7–8 weeks) were immunized subcutaneously with 50 or 200 μg of myelin oligodendrocyte glycoprotein (MOG_{35-55}; MEVGWYRSPFSRVVHLYRNGK) (GLBiochem, Shanghai, China) in 100 μl of a solution containing 50% of complete Freund's adjuvant with 10 mg/ml heat-killed H37Ra strain *Mycobacterium tuberculosis* (Difco) into areas draining into axillary and inguinal lymph nodes. Pertussis toxin (List Biological Laboratories, Campbell, CA) in phosphate-buffered saline (PBS; at 200 ng/mouse) was administered intraperitoneally on days of immunization and again 48 h later. Animals were weighed and examined for disease symptoms daily. Evaluation of disease severity and other experiments were carried out in a blinded fashion. Disease severity was scored using a scale 0–5 as follows: 0 = no symptom; 1 = limp tail; 2 = weakness and incomplete paralysis of one or two hind limbs; 3 = complete hind limb paralysis; 4 = forelimb weakness or paralysis; 5 = moribund state or death.

Histological Analysis—Mice were anesthetized with diethyl ether, transcardially perfused with cold saline, and perfused with 4% paraformaldehyde diluted in 0.1 M PBS. Lumbar spinal cords were fixed using 4% paraformaldehyde for 3 days and then cryo-protected with 30% sucrose solution for 3 days. Three animals were used per experimental group. Fixed brains were embedded in OCT compound (Tissue-Tek, Sakura Finetek, Japan) for frozen sections and then sectioned coronally at 20 μm. Sections were stained with hematoxylin and eosin (H&E) to assess inflammatory lesions. To detect LCN2 expression, demyelination, glial activation, and immune cell infiltration sections were incubated with goat anti-LCN2 antibody (1:500 dilution; R&D Systems, Minneapolis, MN), fluoromyelin (1:300 dilution; Invitrogen), mouse anti-GFAP antibody (1:500 dilution; BD Bioscience), rabbit anti-Iba-1 antibody (1:500 dilution; WAKO Osaka, Japan), and rat anti-CD4 antibody (1:200 dilution; Serotec, Oxford, UK). Sections were visualized directly or incubated with FITC-conjugated anti-mouse, rat, rabbit, or goat IgG antibody (The Jackson Laboratory, Bar Harbor, ME) or Cy3-conjugated anti-goat IgG antibody (The Jackson Laboratory). Percentage of LCN2- or 24p3R-expressing cells was determined by quantification of fluorescence intensities using Image J software and co-localization plug-in. For the quantification of demyelination, images of the lumbar sections were obtained, and Image J software was used to outline the demyelination area and total white matter area. Pixel area for each sample was calculated, and the percentage of demyelination was determined by dividing the total white matter area by the total demyelinated area (three lumbar sections examined for each animal). Histological scores were evaluated using H&E-stained lumbar spinal cord sections and the following scale (51): 0 = no infiltration; 1 = mild infiltration around pial vessels; 2 = single-cell infiltration within the CNS; 3 = infiltration with mild perivascular cuffing; 4 = very intense infiltration with perivascular cuffing. For double-immunofluorescence

TABLE 1
DNA sequences of the primers used for traditional and real-time RT-PCR

Genes	RT-PCR methods	GenBank™ accession no.	Primer sequences
Lipocalins			
Lcn2	Traditional	NM_008491	F: 5′-ATG TCA CCT CCA TCC TGG TC-3′
			R: 5′-CAC ACT CAC CAC CCA TTC AG-3′
Lcn2	Real time	NM_008491	F: 5′-CCC CAT CTC TGC TCA CTG TC-3′
			R: 5′-TTT TTC TGG ACC GCA TTG G-3′
MMPs			
Mmp9	Real time	NM_013599	F: 5′-AAT CTC TTC TAG AGA CTG GGA AGG AG-3′
			R: 5′-AGC TGA TTG ACT AAA GTA GCT GGA-3′
Mmp2	Real time	NM_008610	F: 5′-CAG GGA ATG AGT ACT GGG TCT ATT-3′
			R: 5′-ACT CCA GTT AAA GGC AGC ATC TAC-3′
Cytokines			
Il1b	Real time	NM_008361	F: 5′-AGT TGC CTT CTT GGG ACT GA-3′
			R: 5′-TCC ACG ATT TCC CAG AGA AC-3′
Il6	Real time	NM_031168	F: 5′-AGT TGC CTT CTT GGG ACT GA-3′
			R: 5′-TCC ACG ATT TCC CAG AGA AC-3′
Il12	Real time	M86672	F: 5′-CAT CGA TGA GCT GAT GCA GT-3′
			R: 5′-CAG ATA GCC CAT CAC CCT GT-3′
Il17a	Real time	NM_010552	F: 5′-GAA GCT CAG TGC CGC CA-3′
			R: 5′-TTC ATG TGG TGG TCC AGC TTT-3′
Ifng	Real time	NM_008337	F: 5′-TGC TGA TGG GAG GAG ATG TCT-3′
			R: 5′-TTT CTT TCA GGG ACA GCC TGTT-3′
Tnf	Real time	NM_013693	F: 5′-ATG GCC TCC CTC TCA GTT C-3
			R: 5′-TTG GTG GTT TGC TAC GAC GTG-3′
Chemokines			
Ccl2	Real time	NM_011333	F: 5′-TCA GCC AGA TGC AGT TAA CG-3′
			R: 5′-GAT CCT CTT GTA GCT CTC CAG C-3′
Cxcl10	Real time	NM_021274	F: 5′-AAG TGC TGC CGT CAT TTT CT-3′
			R: 5′-GTG GCA ATG ATC TCA ACA CG-3′
Transcription factors			
Rorc	Real time	AJ132394	F: 5′-TTT GGA ACT GGC TTT CCA TC-3′
			R: 5′-AAG ATC TGC AGC TTT TCC ACA-3′
Tbet	Real time	NM_019507	F: 5′-GGT GTC TGG GAA GCT GAG AG-3′
			R: 5′-GAA GGA CAG GAA TGG GAA CA-3′
Housekeeping genes			
Gapdh	Traditional	NM_008084	F: 5′-ACC ACA GTC CAT GCC ATC AC-3′
			R: 5′-TCC ACC ACC CTG TTG CTG TA-3′
Gapdh	Real time	NM_008084	F: 5′-TGG GCT ACA CTG AGC ACC AG-3′
			R: 5′-GGG TGT CGC TGT TGA AGT CA-3′

staining, sections were incubated with a mixture of rabbit anti-LCN2 antibody (R&D Systems) or anti-24p3R (Slc22A17) antibody (Sigma) and either mouse anti-GFAP antibody (BD Bioscience), rabbit anti-Iba-1 antibody (WAKO), mouse anti-NeuN antibody (1:500 dilution; Millipore, Billerica, MA), rat anti-CD4 antibody (1:200 dilution; Serotec), rat anti-CD45 antibody (1:200 dilution; Santa Cruz Biotechnology, Santa Cruz, CA), rat anti-Ly6G (Gr-1) antibody (1:200 dilution; eBioscience, San Diego, CA), or hamster anti-CD11c antibody (1:200 dilution; eBioscience) overnight at 4 °C. Sections were then incubated with secondary antibody, washed, coverslipped with Vectashield mounting medium (Vector Laboratories, Burlingame, CA), and examined under a confocal microscope. GFAP and Iba-1 fluorescence intensities and numbers of $CD4^+$ T cells were quantified using Image J software. Pictures were taken of three non-overlapping fields of view chosen at random for each experiment. For immunohistochemistry, sections were washed briefly and then incubated with 0.3% H_2O_2 in 0.1 M PBS for 30 min at room temperature to quench endogenous peroxidase activity, permeabilized in 0.1% Triton X-100, and blocked with 1% BSA and 5% normal goat serum. After washing with PBS, the sections were incubated at 4 °C overnight with rabbit polyclonal anti-LCN2 antibody (1:500 dilution; R&D Systems) and then incubated with biotinylated anti-rabbit IgG antibody (1:200 dilution; Vector Laboratories). Sections were then incubated with avidin-biotin complex reagents (Vector Laboratories) for 30 min at room temperature followed by diaminobenzidine detection. The sections were mounted on gelatin-coated slides and allowed to air-dry overnight. Each section was captured using a CCD color video camera (Olympus D70) attached to a microscope (Olympus BX51) equipped with a 100× objective lens.

Traditional or Real-time Reverse Transcription-PCR—Total RNA was extracted from cells or tissues using TRIzol reagent (Invitrogen) according to the manufacturer's instructions. Reverse transcription was conducted using Superscript II (Invitrogen) and oligo(dT) primers. PCR amplification was conducted using a DNA Engine Tetrad Peltier Thermal Cycler (MJ Research, Waltham, MA) at an annealing temperature of 55–60 °C for 20–30 cycles using specific primer sets. To analyze PCR products, 10 μl of each PCR product was electrophoresed on 1% agarose gel and detected under UV light. *Gapdh* was used as an internal control. Real-time PCR was performed using the One Step SYBR® PrimeScript™ RT-PCR kit (Perfect Real-time; Takara Bio Inc., Tokyo), and detection was performed using the ABI Prism® 7500 Sequence Detection System (Applied Biosystems, Foster City, CA). Nucleotide sequences of the primers were based on published cDNA sequences (Table 1).

Cell Proliferation Assay—Spleen cells were cultured at a density of 4×10^5 cells per well in 96-well plates in RPMI 1640 medium (Invitrogen) supplemented with 10% (v/v) fetal bovine serum and 100 units/ml antibiotics. Cells were incubated with MOG_{35-55} peptide (10 μg/ml), proteolipid protein (10 μg/ml), or concanavalin A (5 μg/ml) (Sigma) for 48 h. Cultures were then pulsed with 1 mCi of 8-methylthymidine (specific activity 42 Ci/mmol; Amersham Biosciences) and incubated for an additional 18 h. Cells were harvested, and radioactivities were measured using a liquid scintillation spectrometer (Wallac Micro Beta TriLux, PerkinElmer Life Sciences). Results are expressed as cpm.

In Vitro and in Vivo Treatments with Recombinant LCN2 Protein—Recombinant mouse LCN2 protein expressed in mammalian cells was purchased from R&D Systems. For some experiments, recombinant mouse LCN2 protein expressed as a glutathione *S*-transferase fusion protein in *E. coli* BL21 strain was used (41). For *in vitro* treatment, draining lymph nodes and spleens were collected 10 days after EAE induction. The lymph node and spleen cells (3×10^6 cells/ml) were cultured in complete RPMI medium (Lonza, Walkersville, MD) containing 30 μg/ml MOG_{35-55} with or without 1 μg/ml of recombinant LCN2 protein. After 2 days of culture, RNA was isolated from cell pellets. Primary mixed glial cultures were prepared from the brains of neonatal mice (<2 days old). Cells were cultured in the presence of 0.01~10 μg/ml recombinant LCN2 protein for 6~24 h, and total RNA or culture media were subjected to real-time PCR, ELISA, or gelatin zymography to measure proinflammatory cytokine, chemokine, and matrix metalloproteinase levels. For *in vivo* LCN2 injections, recombinant LCN2 protein or its denatured form was administered intrathecally (5 and 50 ng daily from 7 to 11 days) or intraperitoneally (10 μg daily for 2 weeks) to mice after MOG immunization. Animals were weighed and examined daily for disease symptoms.

Adoptive Transfer of EAE—For adoptive transfer, WT or *Lcn2*-deficent mice were immunized with MOG_{35-55}, complete Freund's adjuvant, and pertussis toxin. Lymph nodes and spleens were collected 10 days later. Draining lymph nodes and spleen cells were cultured in complete RPMI medium containing 30 μg/ml MOG_{35-55} at 1×10^7 cells/ml. After 3 days of culture, cells were harvested and washed with Hanks' balanced salt solution and then transferred intravenously to irradiated (400 rads) WT or *Lcn2* KO mice. Animals were weighed and examined daily for symptoms of disease.

Statistical Analysis—All values are expressed as the mean ± S.E. Student's *t* test was used to determine the statistical significance of LCN2 mRNA, protein expression, histological score, and demyelination percentage in tissues. EAE scores and categorical variables were analyzed by the Mann-Whitney nonparametric test. Results of adoptive transfer experiment were analyzed by one-way and two-way ANOVA with Bonferroni's post-hoc test. All other data sets were analyzed by one-way or two-way ANOVA with Bonferroni's post-hoc tests using SPSS Version 14.0 K (SPSS Inc., Chicago, IL). Statistical significance was accepted for p values < 0.05.

RESULTS

LCN2 Levels in Peripheral Immune Organs and in Spinal Cords after EAE Induction—To determine the role played by LCN2 in autoimmune neuroinflammation, we first investigated LCN2 expression in an EAE mouse model. C57BL/6 mice were immunized by subcutaneous injection of MOG peptide emulsified in complete Freund's adjuvant followed by intraperitoneal injections of pertussis toxin on days 0 and 2 after EAE induction. In non-immunized naïve mice, *Lcn2* mRNA was barely detected in spinal cords and not detected in lymph nodes or spleen cells. However, after EAE induction, *Lcn2* expression was markedly increased in spinal cords and in secondary immune organs (Fig. 1, *A* and *B*). Days 10 and 17 after EAE induction were selected as time points for *Lcn2* expression analysis in the spinal cord and in peripheral lymphoid organs, respectively; these values were chosen based on peak times for encephalitogenic immune responses in the spinal cord and peripheral lymphoid organs (52). Immunofluorescence was then used to evaluate LCN2 protein expression in spinal cords and peripheral immune organs. In spinal cords, LCN2 expression was very low in the gray matter of treatment naïve mice. However, after EAE induction, strong LCN2 expression was observed, mostly in the white matter of spinal cords (Fig. 1*C*). Similarly, LCN2 protein expression was also elevated in lymph nodes and spleens after EAE induction (Fig. 1*D*). These results led us to hypothesize that LCN2 may be involved in EAE pathogenesis.

LCN2 Expression in EAE-induced Spinal Astrocytes and Spleen Neutrophils—In our previously studies, we found *Lcn2* gene expression was up-regulated and that LCN2 protein was secreted by microglia and astrocytes under inflammatory conditions (41, 42). Subsequent studies by others also demonstrated glial expression of LCN2 in the CNS (44, 46, 53). Thus, we examined whether glial cells and neurons in the spinal cord express LCN2 during EAE. Mice were immunized with MOG peptide and pertussis toxin, and spinal cords were isolated during the disease peak and chronic phases (17 and 30 days after EAE induction, respectively). The spinal cord sections were subjected to double-immunofluorescence staining with LCN2 antibody and either GFAP (an astrocyte marker), Iba-1 (a microglia/macrophage marker), or NeuN (a neuron marker) antibodies. LCN2 was highly expressed in the $GFAP^+$ astrocytes, but not microglia or neurons, at the disease peak (Fig. 2, *A–C*), and astrocytes maintained a high level of LCN2 expression in the chronic phase (data not shown). The expression of LCN2 in $GFAP^+$ astrocytes was also observed in cerebellum at the disease peak (data not shown). Because LCN2 expression was also increased in peripheral immune organs after EAE induction (Fig. 1), we next investigated the localization of LCN2 protein within spleens and lymph nodes. Spleen sections were stained with LCN2, CD4 (T cell marker), CD45 (macrophage marker), CD11c (dendritic cell marker), or Ly6G (neutrophil marker) antibodies 10 days after EAE induction, and LCN2 was found to be expressed in neutrophils, but not in T cells, macrophages, or dendritic cells, in the spleens and lymph nodes of EAE-induced mice (Fig. 2*D*). These findings suggest that LCN2 expressed in astrocytes and neutrophils plays an important role

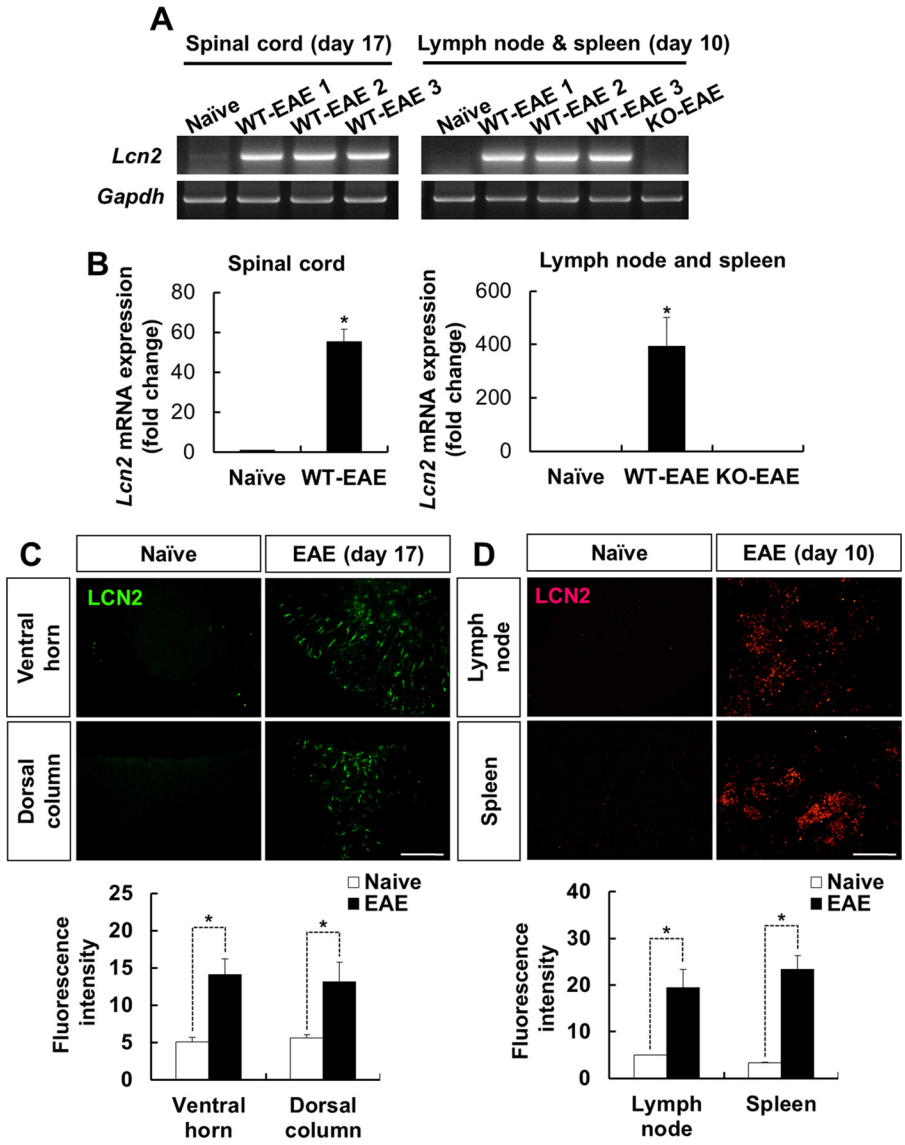

FIGURE 1. **LCN2 expression was up-regulated in EAE-induced mice.** WT ($n = 3$) and *Lcn2* KO ($n = 3$) mice were immunized with MOG peptide and pertussis toxin. At days 10 and 17 after EAE induction, spinal cords, lymph nodes, and spleens were removed. Total RNAs were isolated, and the mRNA levels of LCN2 were determined by traditional RT-PCR (*A*) and real-time PCR (*B*). *Gapdh* was used as an internal control. *, $p < 0.01$, naïve *versus* EAE (Student's *t* test). Results for individual animals and representative results are shown for WT and *Lcn2* KO mice, respectively. Spinal cord, lymph node, and spleen tissue sections derived from naïve and EAE-induced mice were stained with anti-LCN2 antibody and secondary FITC- or Cy3-conjugated anti-goat IgG antibody for immunofluorescence analysis (*C* and *D*). *Scale bar* = 200 μm. Results are representative of more than three independent experiments. Quantification of fluorescence intensities revealed that LCN2 expression was increased in the spinal cords, spleen, and lymph node of EAE-induced mice compared with naïve mice (*graphs*). Results are the mean ± S.E. ($n = 3$). *, $p < 0.01$, naïve *versus* EAE (Student's *t* test).

in inflammatory responses in the CNS and periphery, respectively, under autoimmune conditions.

24p3R Expression in the Spinal Cord and Periphery during EAE—To determine whether CNS-resident cells and peripheral immune cells express LCN2 receptor 24p3R, spinal cords (17 after EAE induction) and spleen (day 10 after EAE induction) were harvested from EAE-induced mice. Immunofluorescence staining showed that astrocytes and microglia expressed high levels of 24p3R (Fig. 2*E*). Spinal neurons did not express 24p3R at the disease peak. In spleen tissues 24p3R was mainly expressed in $CD11c^+$ cells (dendritic cells and activated T cells) (54) at pre-symptomatic phase (day 10 after EAE induction) (Fig. 2*F*). In addition, 24p3R-expressing $CD4^+$ T cells were identified in spinal cord as well (Fig. 2*E*). These results suggest that LCN2 protein, secreted during EAE development, may act on astrocytes, microglia, and CNS-infiltrating T cells in spinal cords and on dendritic cells and T cells in spleen.

Lcn2-deficient Mice Exhibited EAE with a Delayed Course and Reduced Severity—To investigate the potential role of LCN2 in the initiation and progression of EAE, disease onset times, susceptibilities, and severities were compared in WT and *Lcn2* KO mice after injecting 50 μg (to induce mild EAE) or 200 μg (to induce severe EAE) of MOG peptide and pertussis toxin. In WT mice, severe disease symptoms, such as limping and tail and limb paralysis, were observed with a maximum EAE score at ~15 days after EAE induction with 200 μg of MOG peptide (maximum EAE score, 2.75 ± 0.13). *Lcn2* KO mice showed less severe symptoms (maximum EAE score, 1.66 ± 0.22) (Fig. 3*A*,

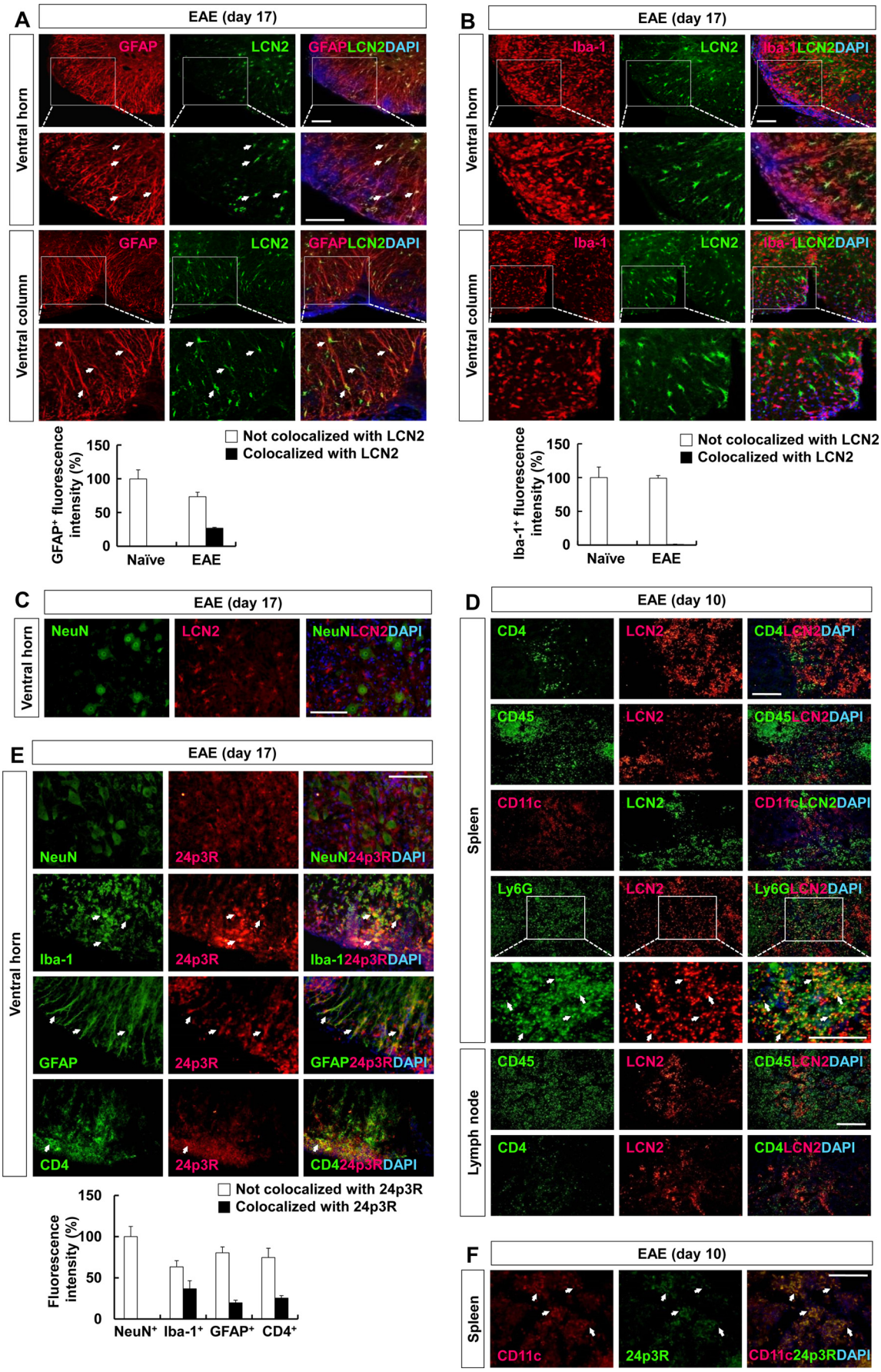
A
EAE (day 17)
Ventral horn
Ventral column
GFAP
LCN2
GFAPLCN2DAPI
Not colocalized with LCN2
Colocalized with LCN2
GFAP+ fluorescence intensity (%)
150
100
50
0
Naïve
EAE
B
EAE (day 17)
Iba-1
Iba-1LCN2DAPI
Iba-1+ fluorescence intensity (%)
C
EAE (day 17)
NeuN
NeuNLCN2DAPI
D
EAE (day 10)
Spleen
Lymph node
CD4
CD45
CD11c
Ly6G
CD4LCN2DAPI
CD45LCN2DAPI
CD11cLCN2DAPI
Ly6GLCN2DAPI
E
EAE (day 17)
24p3R
NeuN24p3RDAPI
Iba-124p3RDAPI
GFAP24p3RDAPI
CD424p3RDAPI
Not colocalized with 24p3R
Colocalized with 24p3R
Fluorescence intensity (%)
NeuN+ Iba-1+ GFAP+ CD4+
F
EAE (day 10)
CD11c24p3RDAPI

left panel). Although the disease incidences were similar in WT and *Lcn2* KO mice, the severity of disease progression was obviously mitigated in *Lcn2* KO mice (Table 2). Furthermore, the percentage of mice that developed hind-limb paralysis after immunization was smaller in *Lcn2* KO mice. In addition, disease onset was delayed in *Lcn2* KO mice as compared with WT mice (day 13 *versus* day 11). In contrast, disease symptoms in WT and *Lcn2* KO mice under the mild condition were not significantly different, although the average EAE score in *Lcn2* KO mice was lower than in WT mice (Fig. 3*A*, *right panel*). Taken together, these findings suggest LCN2 plays a critical role in EAE development. Because it has been shown that the development of EAE is associated with immune cell infiltration and myelin sheath degradation leading to the loss of axonal conduction and EAE symptoms (3–5), we next compared demyelination and immune/inflammatory infiltration in the spinal cords of WT mice and *Lcn2* KO mice at disease peaks. Consistent with the disease score, histological examination of the spinal cords of WT and *Lcn2* KO mice revealed a significant difference. WT mice displayed the characteristic EAE histological alteration, including massive parenchymal lymphocytic infiltration, perivascular cuffing with mononuclear cells, and demyelination in lumbar spinal cord (Fig. 3*B*). Inflammatory cells formed discrete perivascular infiltrate in subpial and parenchymal white matter tracts and consisted of lymphocytes. Macrophages were also observed with myelin globules, which are neutral lipid globules from broken myelin. However, this infiltration of inflammatory cells into the CNS through subpial and perivascular region was minimally detected in the spinal cords of *Lcn2* KO mice. These observations were supported by histological scores and demyelination area percentages (Fig. 3*B*, *graphs*). Furthermore, in the chronic phase, *Lcn2* KO mice showed less inflammatory infiltration (histological score, 1.40 ± 0.54) and demyelination ($3.08 \pm 1.78\%$) than WT animals (histological score, 2.60 ± 0.24; demyelination, $22.13 \pm 5.73\%$).

We next investigated relations between LCN2 and the responses of resident glial cells in the CNS during EAE. Increased numbers of $GFAP^+$ astrocytes and $Iba\text{-}1^+$ microglia were observed at the disease peak (day 17 after EAE induction) by immunofluorescence staining of the spinal cords of WT mice (Fig. 4, *A* and *B*), and these increases were attenuated in *Lcn2* KO mice. In addition, prolonged monitoring of spinal cord sections for up to 30 days after EAE induction revealed a continuous difference between glial activation in WT and *Lcn2* KO mice in the chronic disease stage (data not shown). These results suggest that LCN2 is required for the activation of astrocytes and microglia during the development and progression of EAE.

Lcn2 KO Mice Exhibited Less Leukocyte Infiltration into Spinal Cords—The infiltration of effector T cells is a critical process for the induction of CNS inflammation and the pathology of EAE. Thus, we compared accumulation of T cell populations in the spinal cords of WT and *Lcn2* KO mice after EAE induction. $CD4^+$ T cells influx into spinal cords was observed in WT mice, whereas $CD4^+$ T cells were less abundant in the spinal cords of *Lcn2* KO mice (Fig. 4*C*). These results indicate that the absence of *Lcn2* leads to diminished CNS infiltration by effector T cells and reduced demyelination and subsequent axonal injury.

Lcn2 Deficiency Diminished the mRNA Expression of Inflammatory Cytokines and Chemokines during EAE—To determine whether *Lcn2* deficiency affects the expression of proinflammatory genes in spinal cords during EAE, quantitative real-time RT-PCR was performed to assess the expression levels of inflammatory cytokines and chemokines. At day 17 after EAE induction, the mRNA expression of proinflammatory cytokines and chemokines (*Il17a*, *Ifng*, *Tnf*, *Il12*, *Il6*, *Il1b*, *Ccl2*, and *Cxcl10*) was strongly enhanced in the spinal cords of WT mice, and this enhancement was significantly less in spinal cords of *Lcn2* KO mice. In particular, EAE-induced *Il17a* and *Ifng*, which are known to be produced by Th17 and Th1 cells, respectively, were expressed at significantly lower levels in the spinal cords of *Lcn2* KO mice (Fig. 5*A*). Furthermore, EAE-induced proinflammatory cytokines (*Tnf*, *Il6*, and *Il1b*) and chemokines (*Cxcl10*) were also expressed at lower levels in *Lcn2* KO mice 30 days after EAE induction, whereas *Il12* was expressed at similar levels in WT and *Lcn2* KO spinal cords (data not shown). These results were consistent with the histological finding that the absence of the *Lcn2* gene was associated with reduced spinal cord inflammation. To determine how *Lcn2* deficiency influences peripheral immune response, proinflammatory cytokine gene expression in lymph nodes and spleens were compared in WT and *Lcn2* KO mice. The EAE-induced expression of *Il17a*, *Ifng*, and *Il6* in secondary lymphoid tissues was found to be significantly lower in *Lcn2* KO mice than in WT mice (Fig. 5*B*). These results indicate that LCN2 expression is essential for the induction of inflammatory mediators in peripheral immune organs and in the CNS during EAE. In addition, we asked whether *Lcn2* deficiency affects the proliferative ability of MOG-specific T cells in peripheral lymphoid tissue at disease peaks. We found that autoreactive T cells from *Lcn2* KO EAE mice showed significantly lower levels of proliferation than WT EAE mice when restimulated in the presence of MOG peptide (Fig. 5*C*). However, no significant difference was found after restimulation with a control proteolipid protein (one of the three major myelin proteins). Next, we compared the sizes of lymph nodes and spleens of WT and *Lcn2* KO mice. WT mice

FIGURE 2. **LCN2 and 24p3R expression in spinal cords, spleens, and lymph nodes during EAE.** Frozen sections of lumbar spinal cords, spleens, and lymph nodes were prepared from EAE-induced mice at peak disease severity (day 17; $n = 3$) or during the pre-symptomatic phase (day 10; $n = 3$) and subjected to immunofluorescence analysis and confocal microscopy to localize LCN2 (*A–D*) and 24p3R (its receptor) (*E* and *F*) immunoreactivity in several cell types; that is, in astrocytes, microglia, neurons, T cells, macrophages, dendritic cells, and neutrophils. *Arrows* indicate the co-localization of LCN2 or 24p3R and cell type-specific markers. *Scale bars* = 100 μm. Quantification of LCN2 or 24p3R fluorescence intensity was carried out by determining the percent co-localization of LCN2 or 24p3R and cell type-specific markers (*graphs*). GFAP, astrocyte-specific marker; Iba-1, microglial cell marker; NeuN (neuronal marker); CD4 (T cell marker); CD45 (macrophage marker); CD11c (dendritic cell marker); Ly6G (neutrophil marker). Nuclei were stained with DAPI (4,6-diamidino-2-phenylindole; *blue*). Images are representative of three independent experiments.

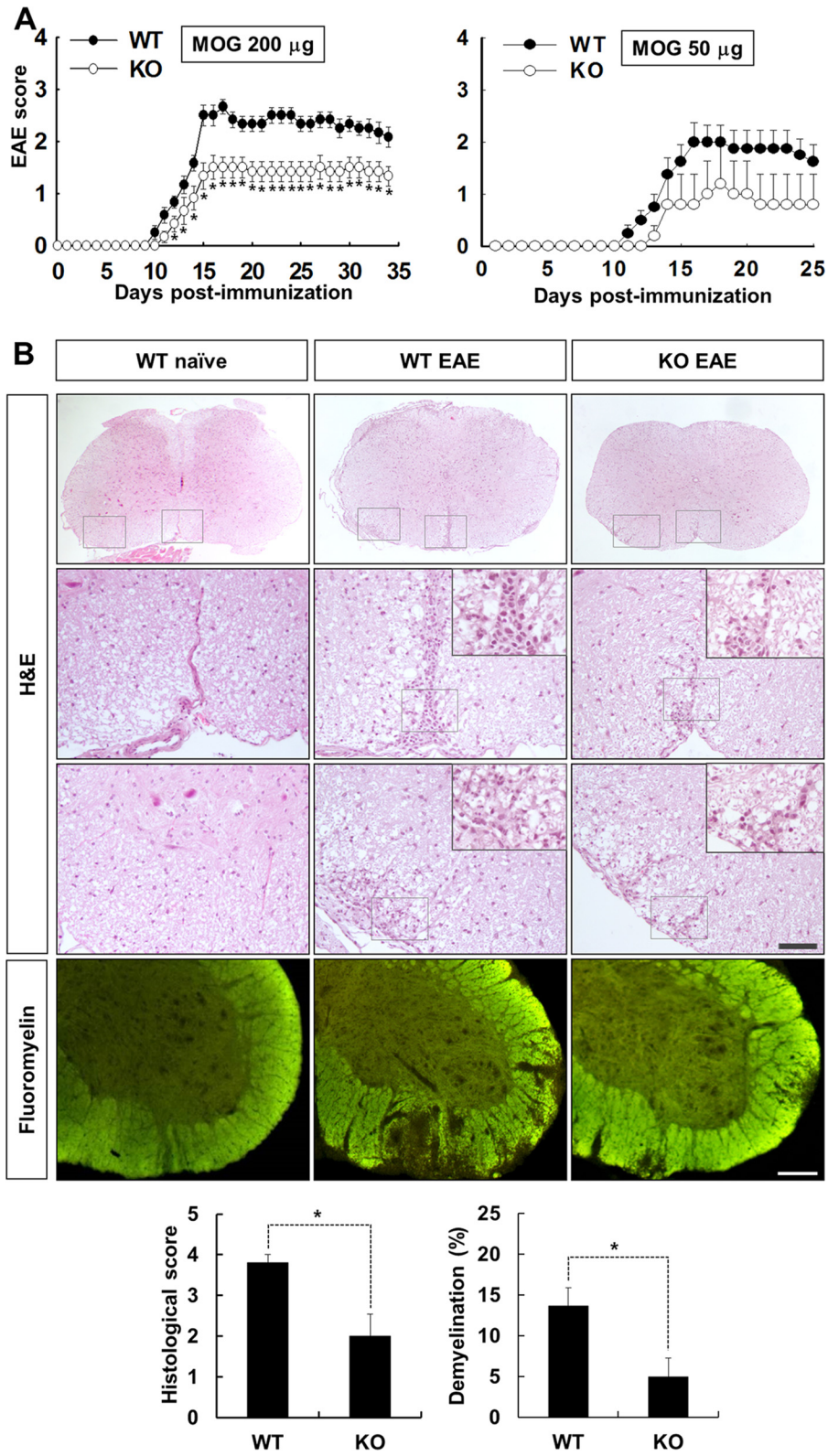

FIGURE 3. **Reduction of EAE pathology and disease severity in *Lcn2*-deficient mice.** WT and *Lcn2* KO mice were immunized with MOG peptide at doses of 200 μg ($n = 12$ per group) or 50 μg ($n = 5$ per group) with complete Freund's adjuvant and pertussis toxin. The immunized mice were observed daily for 35 days (*A*, *left*) or 25 days (*A*, *right*) to determine mean EAE scores. Disease severity was significantly less in *Lcn2* KO mice than in WT mice after injecting 200 μg of MOG (*A*, *left*), but no significant difference was found between WT and KO mice after injecting 50 μg of MOG (*A*, *right*). Results are the mean ± S.E. *, $p < 0.05$, WT *versus Lcn2* KO mice (Mann-Whitney *U* test). Frozen sections of lumbar spinal cords from non-immunized naive mice or EAE-induced WT or KO mice taken at day 17 after EAE induction were stained with H&E or fluoromyelin (*B*). *Scale bars* = 200 μm. Inflammatory infiltration (*B*, *upper*) and demyelination (*B*, *lower*) were greater in WT-EAE spinal cord white matter than in non-immunized WT controls but significantly less in the spinal cords of *Lcn2* KO-EAE mice than in WT-EAE animals. Inflammatory infiltration and demyelination were quantitatively assessed in the spinal cords of WT and KO mice (*B graphs*). The results are the mean ± S.E. ($n = 5$). *, $p < 0.05$, WT *versus Lcn2* KO mice (Student's *t* test).

TABLE 2
EAE progression in wild-type and *Lcn2*-deficient mice
Results are cumulative data from two different experiments.

Mouse genotype	Incidence	Day of onset	Development of complete hind-limb paralysis	Maximum EAE score
		Mean ± S.E.	*%*	*Mean ± S.E.*
$Lcn2^{+/+}$	12/12 (100%)	11.41 ± 0.35	75.0	2.75 ± 0.13
$Lcn2^{-/-}$	12/12 (100%)	13.16 ± 0.42[a]	8.3[a]	1.66 ± 0.2[a]

[a] $p < 0.05$ as compared to $Lcn2^{+/+}$ animals. p values calculated by Mann-Whitney U test.

showed enlarged lymph nodes and spleens at 10 days after EAE induction, whereas *Lcn2* KO mice exhibited lesser enlargements (Fig. 5*D*). This result was consistent with the lower expression of proinflammatory cytokines observed in the lymph nodes and spleens of *Lcn2* KO mice.

LCN2 Treatment in Vitro Increased MOG-specific T Cell and Glial Cell Responses—To determine the effect of LCN2 on the activation of peripheral immune cells, we examined the effect of LCN2 on the expression of *Il17a* and *Ifng* in MOG-specific T cells. WT and KO mice were immunized with MOG and pertussis toxin, and lymph node and spleen cells were isolated 10 days after immunization. These cells were then cultivated with MOG peptides in the presence or absence of recombinant LCN2 protein (1 μg/ml). MOG-induced *Il17a* and *Ifng* expression was significantly increased by treatment with recombinant LCN2 protein in lymph nodes and spleen cells (Fig. 6, *A* and *B*). In addition, LCN2 treatment also enhanced the expression of *Rorc* (encoding RORγt) and *Tbet* (encoding T-bet), the signature transcription factors of Th17 and Th1 cells, respectively, in lymph node and spleen cells (Fig. 6, *A* and *B*). Similar results were found in WT and *Lcn2* KO mice, supporting the central role of LCN2 in augmenting the proliferation and activation of encephalitogenic T cells in peripheral lymphoid tissues. We then investigated how LCN2 influences the activation of glial cells in the spinal cord. Primary glial cultures were incubated with recombinant LCN2 protein (0.01∼10 μg/ml), and the expression and secretion of proinflammatory mediators was assessed. When treated with LCN2 protein, glial cultures showed dose-dependent elevation in the expression of *Il1b*, *Tnf*, *Cxcl10*, and *Ccl2* (Fig. 6*C*). The production of TNF-α and CXCL10 proteins by glial cells was also significantly increased in the culture media after treatment with 1–10 μg/ml LCN2 protein (Fig. 6*D*). Because MMPs have been shown to contribute to blood brain barrier disruption and demyelination in MS, we next evaluated the effect of LCN2 on glial MMP expression. LCN2 was found to induce *Mmp9* dose-dependently, but not *Mmp2*, at the mRNA and protein levels in glial cells (Fig. 6, *E* and *F*). Furthermore, the expression of cytokines, chemokines, and MMP-9 was unaffected by denatured LCN2 protein or polymyxin B-pretreated LCN2 protein, which excluded the possibility of LPS contamination of the recombinant LCN2 protein preparation (data not shown). These results suggest that astrocyte-derived LCN2 protein promotes the expression of proinflammatory mediators by activating spinal glial cells in an autocrine or paracrine manner.

LCN2 Expression in the CNS and Periphery and EAE Development—Because LCN2 expression was highly induced in spinal astrocytes and peripheral lymphoid organs after EAE induction, adoptive transfer experiments were performed to determine the pathogenic roles of the CNS and peripheral LCN2 in EAE onset and severity. Draining lymph nodes and spleen cells were harvested from WT and *Lcn2* KO mice on day 10 after EAE induction, restimulated *in vitro* with MOG_{35-55} for 3 days, and then transferred intravenously into naive WT or *Lcn2* KO mice. As was expected, the transfer of WT cells reproduced EAE in WT recipients with an incidence of 100%, a symptom onset of ∼13 days, peak symptom severity on day 19 (EAE score 2.83 ± 0.16), and remission from day 20 (Fig. 7*A*). In contrast, WT recipient mice transferred with *Lcn2* KO cells exhibited reduced disease severity (EAE score 0.50 ± 0.22 at day 19). In addition, disease onset in the KO to WT transfer group was significantly delayed as compared with that in the WT to WT transfer control group. Interestingly, when cells from immunized WT mice were transferred to naive *Lcn2* KO mice, lesser symptoms and delayed onset (day 17.16 ± 0.90) were observed, although mean disease score was similar to that of the WT to WT control group at day 19 (Table 3). These findings show that a lack of *Lcn2* in CNS and peripheral immune tissues ameliorates EAE development. To confirm the role of spinal LCN2 in EAE development, we evaluated the effect of directly injecting recombinant LCN2 protein into the spinal cords on disease symptoms. LCN2 protein (at 5 or 50 ng) was administered intrathecally daily for 5 days (days 7, 8, 9, 10, and 11) after EAE induction. Intrathecal injections of recombinant LCN2 protein were found to accelerate EAE development and to increase disease severity significantly in the acute stage but not to significantly influence peak disease severity (Fig. 7*B*). Mice administered with denatured LCN2 protein as a control developed EAE symptoms on day 12 after EAE induction and peak symptom severity on day 16, whereas recombinant LCN2 protein-injected mice developed EAE symptoms on day 9 and peak symptom severity on day 13 (50 ng of LCN2) or day 14 (5 ng of LCN2) (data not shown). To further examine the role of peripheral LCN2 in the EAE development, intraperitoneal injection of recombinant LCN2 protein was also done. Mice injected with LCN2 showed accelerated onset (day 10.2 ± 0.96) and increased disease severity (EAE score 2.0 ± 0.47 at day 15) compared with control group (onset day 12.0 ± 0.77, EAE score 1.2 ± 0.20). These results indicate that LCN2 expressed in both the CNS and the peripheral tissues plays a critical role during EAE development.

DISCUSSION

LCN2 plays an important role in diverse cellular processes including cell death, survival, migration, invasion, and differentiation. Because we issued our first report on the glial expression of LCN2 (41, 55), several studies have demonstrated the potentially important roles played by LCN2 in the physiology

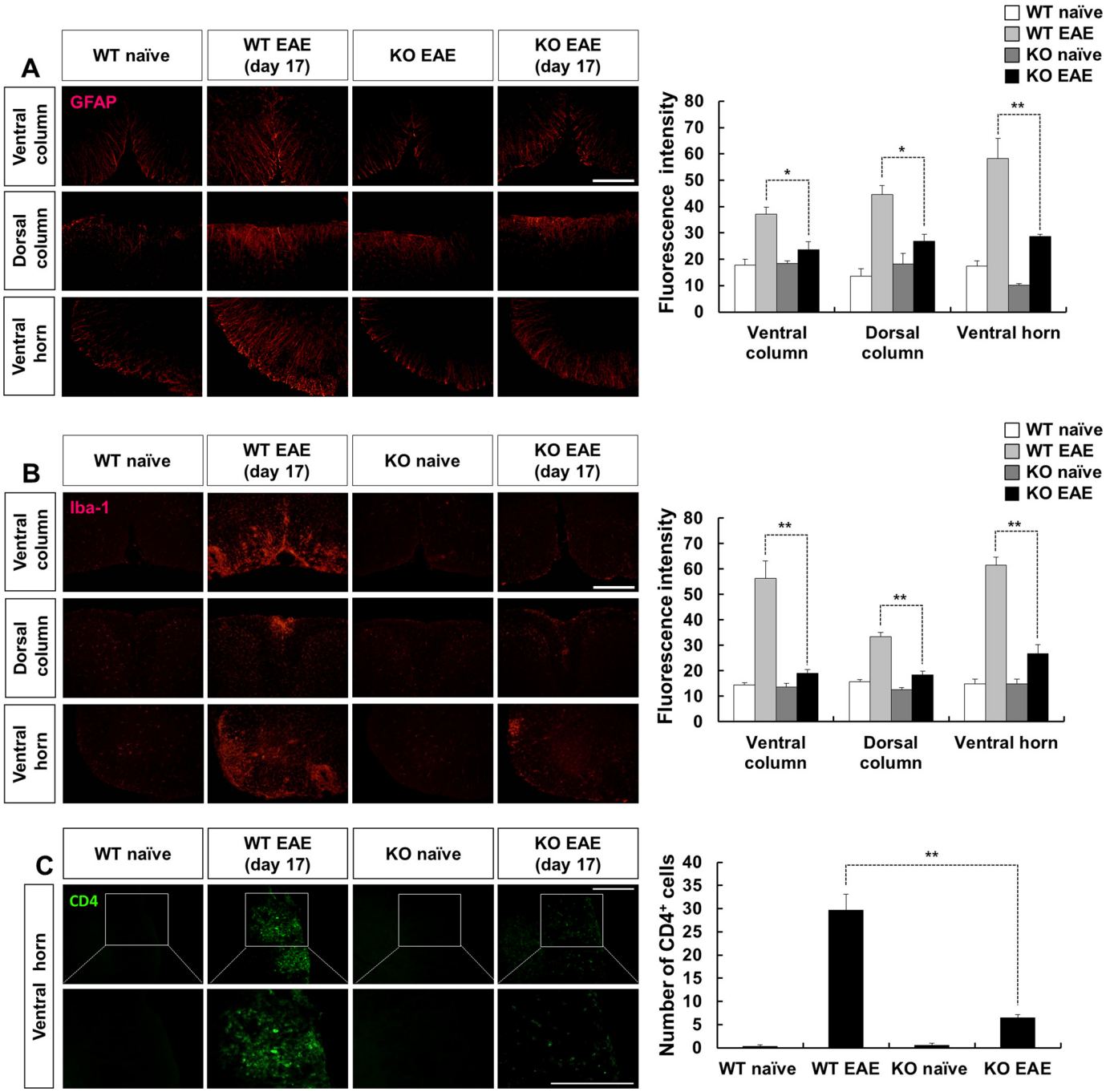

FIGURE 4. **Reduction of EAE-induced glial activation and T cell infiltration in *Lcn2*-deficient mice.** Activation of astrocytes (*A*) and microglia (*B*) at day 17 after EAE induction was assessed by immunofluorescence staining using anti-GFAP and anti-Iba-1, respectively, in lumbar spinal cord sections obtained from treatment naïve or EAE-induced WT or KO mice. Astrocytes and microglia were found to be markedly more activated in EAE-induced WT mice than in naïve controls but to be less activated in EAE-induced KO mice than in WT-EAE animals. In addition, lumbar spinal cord sections obtained from treatment naïve or EAE-induced WT or *Lcn2* KO mice at 17 days after EAE induction were stained with anti-CD4 antibody for immunofluorescence analysis (*C*). *Scale bar* = 200 μm. Quantification of fluorescence intensities or cell numbers revealed that glial activation and T cell infiltration were less in the spinal cords of *Lcn2* KO mice than in WT mice (*graphs*). Results are the mean ± S.E. ($n = 5$) and were analyzed by two-way ANOVA. Genotype x disease significance levels (p value): GFAP ventral column 0.010, dorsal column 0.004, ventral horn 0.015, Iba-1 ventral column 0.000, dorsal column 0.001, ventral horn 0.00, CD4 infiltration 0.000. *, $p < 0.05$, WT EAE *versus* KO EAE in the same spinal cord region (one-way ANOVA with Bonferroni's post-hoc test).

and pathology of the CNS (38, 44, 47, 56). Nevertheless, its functional roles in neuroinflammation and related diseases of the CNS are far from clear, and the results of some previous studies have been contradictory. For example, Ip *et al.* (44) reported no significant difference between inflammatory and glial markers in WT and *Lcn2* KO mice after a peripheral injection of LPS , whereas Rathore *et al.* (46) reported on the detrimental effects of LCN2 after spinal cord injury and on reductions in the expression of several proinflammatory chemokines and cytokines and inducible nitric-oxide synthase after spinal cord injury in *Lcn2* KO mice as compared with WT animals. Furthermore, the proinflammatory effects of LCN2 are supported by our recent findings that LCN2 caused proinflammatory chemokine expression (42) and M1 polarization of micro-

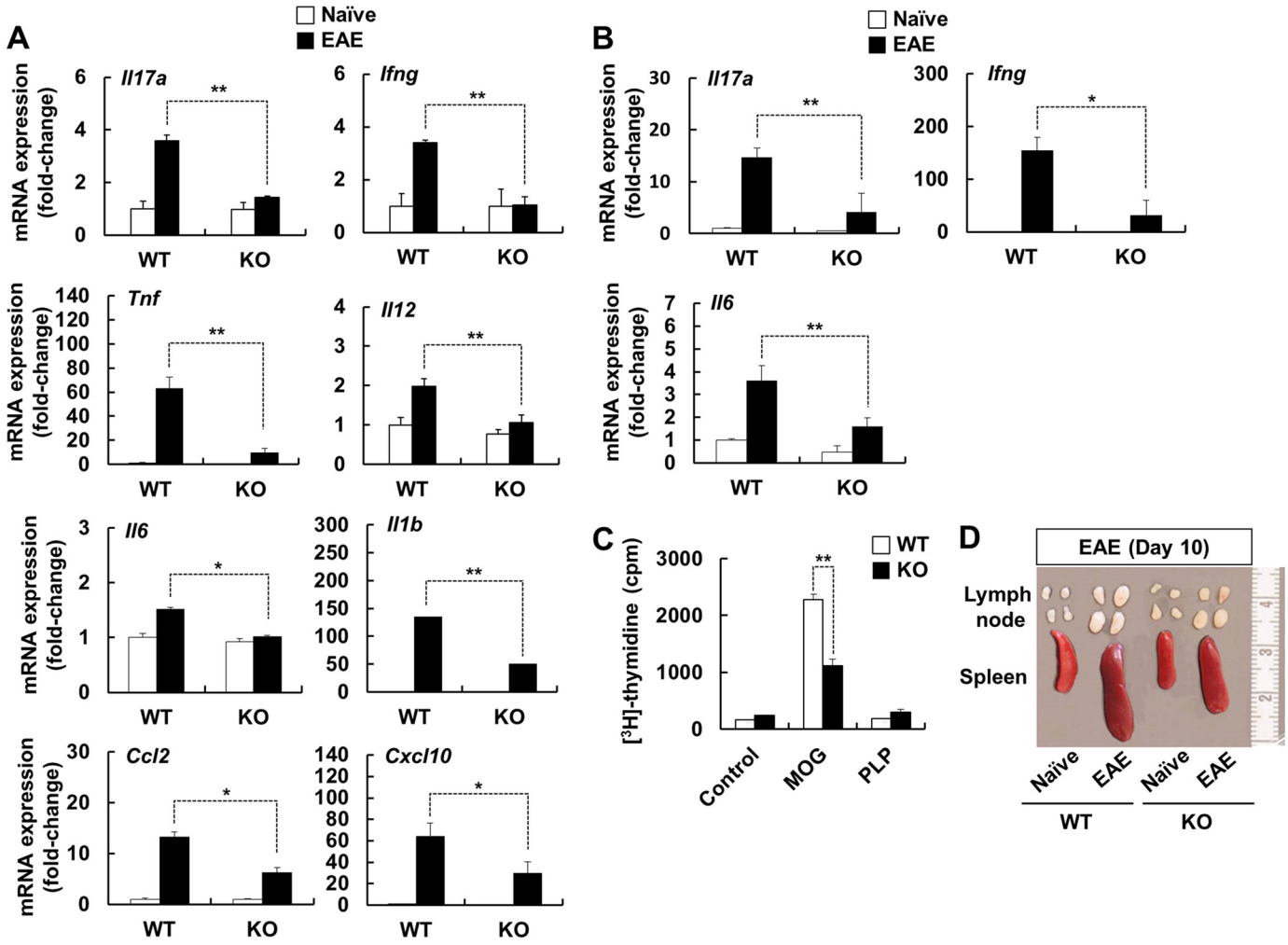

FIGURE 5. **Reduced expression of proinflammatory cytokines and chemokines and the proliferation of autoimmune T cells in *Lcn2* KO mice after EAE induction.** WT and *Lcn2* KO mice were immunized with MOG and pertussis toxin. Spinal cords (at day 17 after EAE induction) (*A*), draining lymph nodes, and spleens (at day 10 after EAE induction) (*B*) were removed, total RNAs were isolated, and the gene expression of inflammatory cytokines and chemokines was determined by real-time PCR. The results shown are the means ± S.E. ($n = 5$) and were analyzed by two-way ANOVA. Genotype x disease significance levels (p value): spinal cord *Il17a* 0.001, *Ifng* 0.004, *Tnf* 0.002, *Il12* 0.003, *Il6* 0.032, *Il1b* 0.021, *Ccl2* 0.041, *Cxcl10* 0.029, lymph nodes and spleen *Il17a* 0.014, *Ifng* 0.014, *Il6* 0.042. *, $p < 0.05$; **, $p < 0.01$ (one-way ANOVA with Bonferroni's post-hoc test). Alternatively, spleen cells from WT and KO mice immunized with MOG and pertussis toxin were cultured in medium alone (control) or in the presence of MOG_{35-55} or proteolipid protein ($PLP_{138-151}$) peptides (*C*). T cell responses were determined by measuring [^{3}H]thymidine incorporation. The results are the mean ± S.E. ($n = 3$) and analyzed by two-way ANOVA. Genotype x treatment significance levels: 0.000. **, $p < 0.01$, WT *versus Lcn2* KO mice (one-way ANOVA with Bonferroni's post-hoc test). Photographs of the spleens and draining lymph nodes of WT and *Lcn2* KO mice at 10 days after EAE induction are shown (*D*).

glia (43). LCN2 has also been proposed as a novel component of proinflammatory signaling in Alzheimer disease (38).

In the present study we report that LCN2 plays a pivotal role in EAE based on the following results: 1) genetic ablation of *Lcn2* significantly attenuated disease severity and reduced inflammatory infiltration, glial activation, inflammatory cytokine/chemokine expression, demyelination, and autoreactive T cell proliferation; 2) LCN2 treatment *in vitro* up-regulated the expression of IL-17 and IFN-γ in MOG-specific T cells and the expression of pro-inflammatory cytokines, chemokines, and neurotoxic molecules in glial cells; 3) intrathecal administration of LCN2 protein during EAE induction caused a dose-dependent shortening of disease onset; 4) adoptive transfer of EAE from WT to KO mice and from KO to WT mice reduced disease severity as compared with WT to WT transfer, indicating that LCN2 expressed in the CNS and peripheral lymphoid tissues plays an important role in EAE development. Furthermore, our results on the localization of LCN2 and its receptor in different cell types indicate that glia-derived LCN2 acts on multiple target cells in the CNS, whereas neutrophil-derived LCN2 primarily acts on dendritic cells in the periphery (Fig. 8).

The present study shows that LCN2 expression is highly up-regulated in spinal astrocytes after EAE induction and that LCN2 secreted by astrocytes mediates inflammatory responses in the EAE spinal cord. Previous studies conducted in our laboratory have demonstrated LCN2 acts as a chemokine inducer in the CNS, mediates reactive astrocytosis, and recruits inflammatory cells to sites of tissue injury or inflammation (41, 42). Astrocyte activation is a prominent feature of CNS pathologies during MS and EAE (57). The present study suggests that *Lcn2* deficiency reduces inflammatory activation of glial cells in the EAE spinal cord and concomitantly attenuates inflammation, and these findings are in line with our previous findings that LCN2 promotes the classical proinflammatory activation of

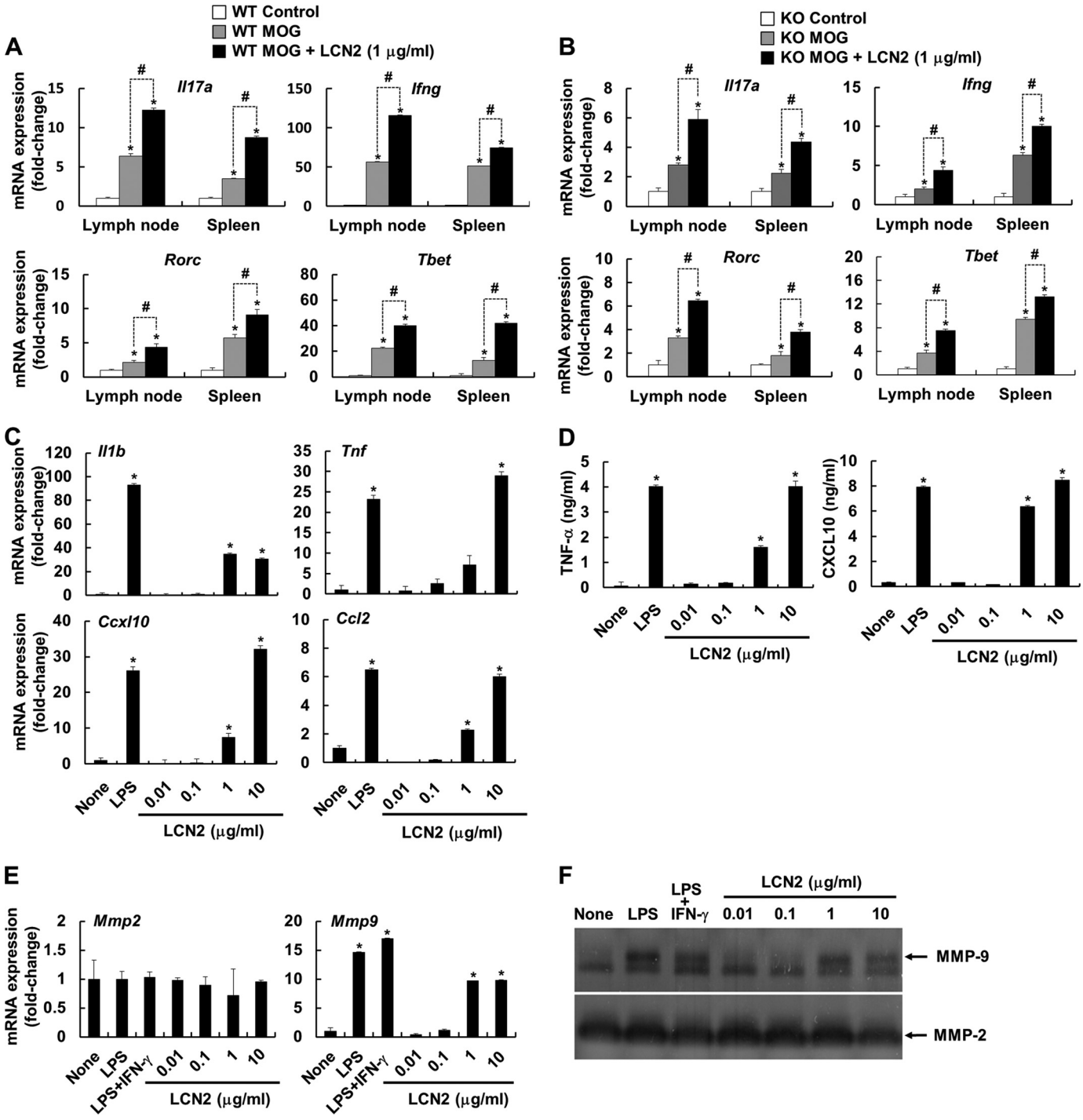

FIGURE 6. **Effect of LCN2 on proinflammatory gene expression in encephalitogenic T cells and glial cells.** At day 10 after EAE induction in WT (*A*) and *Lcn2* KO mice (*B*), lymph node and spleen cells (3×10^6 cells per well) were treated with MOG (30 μg/ml) in the presence or absence of recombinant LCN2 protein (1 μg/ml). Total RNA was isolated after 48 h of MOG re-stimulation. Levels of *Il17a*, *Ifng*, *Rorc*, and *Tbet* mRNA were determined by real-time PCR. Data were normalized *versus Gapdh*, and the results shown are the means ± S.E. ($n = 4$). *, $p < 0.05$ *versus* control; #, $p < 0.05$ between the indicated groups (one-way ANOVA). *C–F*, primary mixed glial cultures were treated with LPS (100 ng/ml) alone, with LPS and IFN-γ (50 units/ml), or with recombinant LCN2 protein (0.01∼10 μg/ml) for 6 h, and total RNA was isolated. The mRNA levels of cytokines (*Il1b* and *Tnf*), chemokines (*Cxcl10* and *Ccl2*) (*C*), and *Mmp2* and *Mmp9* (*E*) were determined by real-time RT-PCR. Amounts of TNF-α and CXCL10 protein (*D*) or MMP proteins (*F*) in culture media were measured by specific ELISA or gelatin zymography, respectively, 24 h after stimulation. mRNA data were normalized *versus Gapdh*. Results are the means ± S.E. ($n = 3$). *, $p < 0.05$ *versus* untreated controls (one-way ANOVA).

microglia (M1 polarization) (43) and astrocytes (41). Previous studies have shown LCN2 induction is associated with many inflammatory conditions in the CNS and peripheral tissues (31, 33, 34, 37, 38, 44, 50), and we have also observed that LCN2 levels in CSF are higher in MS patients than in healthy control subjects (data not shown). The above-mentioned results show that astrocytes and LCN2 play central roles in CNS inflammation during EAE.

Proinflammatory cytokines play central roles in the pathogenesis of MS and EAE via immune system activation and the

recruitment of leukocytes to inflammatory regions (5). In the present study we observed that levels of proinflammatory cytokines, such as, IL-17A, IFN-γ, IL-1β, TNF-α, and IL-6, were markedly lower in *Lcn2* KO mice than in WT animals. IL-17A and IFN-γ, which are produced by Th17 cells and Th1 cells, respectively, play crucial roles in the development and progression of EAE (58). In the CNS, the astrocytic expression of MHC class II molecules is induced by IFN-γ (59) and modulated by TNF-α (60), suggesting that astrocytes are capable of activating T cells via myelin antigen presentation. Astrocytes are also critical in IL-17-Act1-mediated immune cell recruitment during autoimmune-induced inflammation of the CNS (15), which explains the relation between reductions in these proinflammatory cytokine levels in *Lcn2* KO mice and reduced demyelination and inflammatory responses in spinal cords.

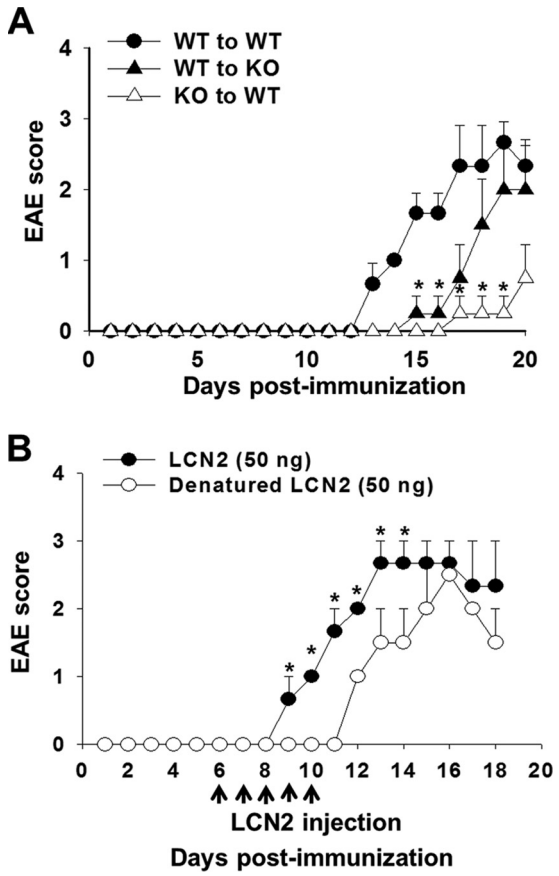

FIGURE 7. **LCN2 expression in the CNS and peripheral immune tissues was required for EAE development.** *A*, WT and *Lcn2* KO mice were primed with MOG peptide and pertussis toxin, and 10 days later lymph nodes and spleen cells were harvested and treated with MOG peptide (30 μg/ml) for 3 days. Restimulated lymph node and spleen cells were injected intravenously into WT ($n = 6$) or *Lcn2* KO ($n = 6$) recipient mice. Results are the means ± S.E. and were analyzed by repeated measures by ANOVA. WT to WT *versus* WT to KO significance, 0.145; WT to WT *versus* KO to WT significance, 0.014. *, $p < 0.05$ *versus* WT to WT transfer (one-way ANOVA with Bonferroni's post-hoc test). *B*, WT mice were immunized with MOG peptide and pertussis toxin. Recombinant LCN2 protein or denatured LCN2 protein was administered intrathecally into mice at 50 ng daily for 5 days (from 7th to 11th days) after EAE induction. Results are the means ± S.E. ($n = 4$). *, $p < 0.05$ *versus* denatured LCN2-injected mice (Mann-Whitney *U* test).

In a previous study we showed that LCN2 secreted by glial cells up-regulates the expression of CXCL10 in the CNS under inflammatory conditions (42), and CCL2 has been shown to be expressed primarily by reactive astrocytes under inflammatory conditions (61–63). Moreover, both of these chemokines are known to play central roles in the inflammatory recruitment of leukocytes and other cell types. In the present study, we found that *Lcn2* deletion reduced the expression of CXCL10 and CCL2 in the CNS, which in turn may have impaired the infiltration of inflammatory cells into the CNS. Furthermore, *Lcn2* deletion reduced the influx of $CD4^+$ T cells into spinal cord parenchyma. We also found that LCN2 induced *Mmp9* at the mRNA and protein levels in cultured glial cells. Interestingly, MMP-9 is up-regulated in MS and in other inflammatory neurodegenerative diseases, and its production has been associated with blood brain barrier damage in EAE model (64). Furthermore, it has been reported MMP-9 levels are elevated at around the time of EAE onset and that the MMP inhibitor GM6001 blocks blood brain barrier breakdown and attenuates disease severity (65). In addition it has been suggested that the interaction between LCN2 and MMP-9 enhances MMP-9 activity by blocking MMP-9 auto-degradation (66, 67). Moreover, MMP-9 is known to be neurotoxic and has been previously associated with neuronal death (68). Interestingly, in an EAE model, genetic ablation of TIMP-1 (tissue inhibitor of metalloproteinase 1, a natural inhibitor of the MMP) was found to increase disease severity (69). Taken collectively, our data suggest that the diminished expression of CXCL10, CCL2, and MMP-9 in *Lcn2*-deficient glial cells probably reduces CNS infiltration by inflammatory cells and demyelination of the EAE spinal cord.

Neutrophils play a key role in the immune system by participating in inflammatory response and adaptive immunity (70). Neutrophils contribute to adaptive immune responses by secreting cytokines to induce the activation of B and T cells (71, 72). Neutrophils are also involved in the differentiation and proliferation of naïve T cells by inducing the activation of antigen presenting cells, such as macrophages and dendritic cells (73). In the present study we identified neutrophils as the major cellular source of LCN2 in peripheral lymphoid tissues after EAE induction. These results suggest that LCN2 secreted by neutrophils may be involved in peripheral immune responses

TABLE 3

EAE progression after adoptive transfer

Results are cumulative data from two different experiments.

Adoptive transfer	Incidence	Day of onset	Development of complete hind-limb paralysis	Maximum EAE score
		mean ± S.E.	%	*mean ± S.E.*
WT to WT	6/6 (100%)	13.33 ± 0.21	83	2.83 ± 0.16
WT to KO	5/6 (83%)	17.16 ± 0.90[a]	50[a]	2.33 ± 0.49[a]
KO to WT	4/6 (66%)	19.00 ± 0.77[a]	0[a]	1.00 ± 0.36[a]

[a] $p < 0.05$ as compared to the WT to WT transfer group. *p* values calculated by Mann-Whitney *U* test.

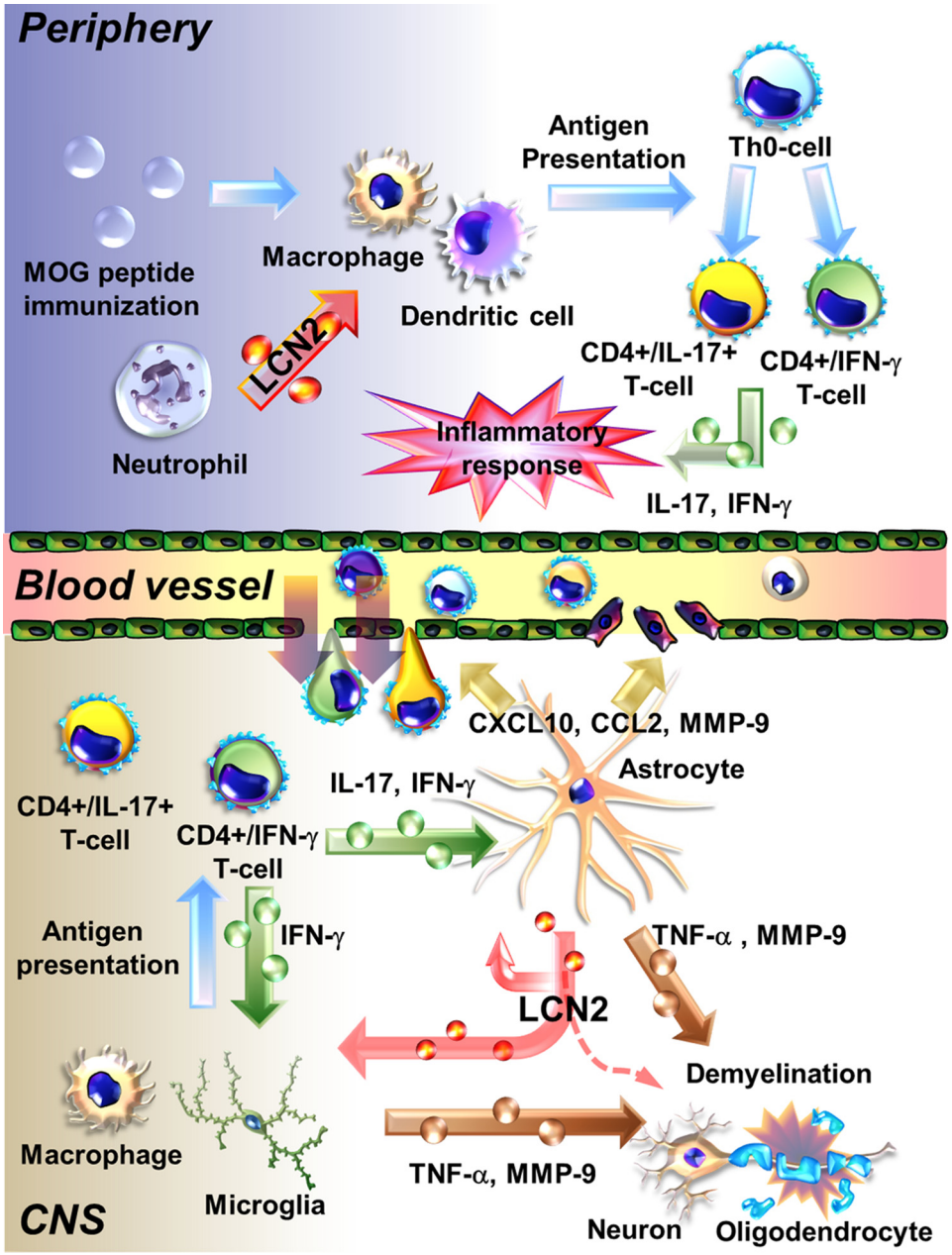

FIGURE 8. **Proposed role of LCN2 in the CNS and peripheral immune system during the development of EAE.** During peripheral immune response to MOG immunization, LCN2 secreted from neutrophils may act on antigen-presenting cells, such as dendritic cells and macrophages, and thereby lead to the differentiation and proliferation of T cells toward proinflammatory IFN-γ-producing Th1 and IL-17-producing Th17 cells. In the CNS, infiltrating T cells may activate CNS-resident astrocytes and microglia. LCN2 secreted by activated astrocytes then promotes the production of proinflammatory mediators by astrocytes and microglia/macrophages in an autocrine or paracrine manner. Glia-derived CXCL10, CCL2, TNF-α, and MMP-9 may initiate and amplify CNS inflammatory infiltration and demyelination.

during EAE. In the present study the expression of the LCN2 receptor, 24p3R, was detected in dendritic cells of the EAE spleen, which suggested that neutrophil-derived LCN2 acts on dendritic cells to influence the antigen presentation process in peripheral lymphoid organs during EAE. This finding is consistent with the previous observation of 24p3R expression in different tissues, such as, spleen, kidney, liver, and lung (28). We also found that the degree of T cell proliferation was lower after the *in vitro* MOG re-stimulation of *Lcn2* KO spleen cells compared with WT cells. In addition, LCN2 increased the mRNA expression of *Rorc* and *Tbet* in MOG-restimulated lymph node cells or spleen cells. *Rorc* and *Tbet* are transcription factors that are associated with the polarizations of Th17 and Th1 cells, respectively, which are critical steps in production of specific cytokines and in the differentiation of naïve T cells to effector T cells (3). Thus, LCN2 secreted by neutrophils in the peripheral immune system appears to be involved in the differentiation, proliferation, and activation of T cells under EAE conditions by directly acting on T cells or by indirectly acting on dendritic cells and other antigen presenting cells.

During the preparation of this manuscript, two studies on the role of LCN2 in EAE development were published. Having previously demonstrated the detrimental effects of LCN2 in a spinal cord injury model (46), the same research group reported

that *Lcn2* KO mice displayed a more severe EAE phenotype than WT animals (74). In another study by Marques *et al.* (75) on the EAE brain, LCN2 expression was found to be increased in EAE, particularly in brain regions typically affected in patients with MS. In the study by Berard *et al.* (74), immunization of C57BL/6 mice with 50 μg of MOG peptide induced both chronic and relapsing-remitting EAE. In this study, although the percentage of animals that developed chronic disease was higher for *Lcn2* KO mice than for the WT, the percentages of animals that died or were sacrificed due to disease severity were not significantly different (74). Furthermore, mean disease onset time and mean EAE score at disease peak for chronic EAE animals were not significantly different between WT and KO mice. However, disease severity was significantly different only for mice with relapsing-remitting characteristics. During the initial stage of the present study, 200 μg of MOG peptide was injected to induce EAE, and *Lcn2* KO mice showed a less severe disease phenotype and had lower mean EAE scores than WT animals. Later, we injected animals with 50 μg of MOG peptide to induce a mild disease condition, in which the disease severities of WT and *Lcn2* KO mice were similar, although it should be added that *Lcn2* deficiency reduced mean EAE scores. Accordingly, our results support the notion that LCN2 plays a pathogenic role in EAE but that its role in the disease process may be less important under mild conditions, which is at odds with the previously reported protective role of LCN2 in EAE. We do not have a clear explanation for this discrepancy. Nonetheless, the study by Berard *et al.* (74) showed a significant up-regulation of LCN2 in the spinal cord throughout EAE, which is consistent with our observations. Marques *et al.* (75) also reported LCN2 levels were increased in the EAE brain and that neutrophil and astrocyte LCN2 expression was observed during the onset and relapse phases in the brains of proteolipid protein-induced SJL mouse model. Furthermore, these authors also found natalizumab (an integrin inhibitor) down-regulated the expression of LCN2 and ameliorated disease severity and that LCN2 CSF levels were correlated with EAE progression (75). These findings of Marques *et al.* (75) concur with the findings of the present study. Indirect evidence also indicates that LCN2 is potentially involved in the development of EAE, as upstream or downstream signaling events associated with LCN2 have been implicated in EAE development. The complement components C3 and C5 are important for the recruitments of inflammatory cells under physiological conditions and in several acute and chronic inflammatory diseases (76, 77). In particular, component C3 mediates LCN2 expression in the spleen-resident immune cells of mice. In C3-deficient mice, EAE severity was attenuated and the infiltrations of macrophages and T cells into CNS parenchyma were reduced (78, 79). LCN2 expression is controlled by IL-6-gp130 signaling pathway during the early inflammatory response (80), and EAE severity was reported to be reduced in gp130 KO mice (81). These previous reports and the present study suggest that LCN2 has a proinflammatory disease-promoting effect during EAE development.

In summary, our findings show LCN2 plays a critical role in inflammatory responses involving reactive astrocytes within the CNS and in the activation of T cells in peripheral immune tissues during EAE development and progression. Accordingly, we advocate that LCN2 be regarded a novel target for the diagnosis and treatment of MS.

REFERENCES

1. Frohman, E. M., Racke, M. K., and Raine, C. S. (2006) Multiple sclerosis: the plaque and its pathogenesis. *N. Engl. J. Med.* **354,** 942–955
2. Man, S., Ubogu, E. E., and Ransohoff, R. M. (2007) Inflammatory cell migration into the central nervous system: a few new twists on an old tale. *Brain Pathol.* **17,** 243–250
3. McFarland, H. F., and Martin, R. (2007) Multiple sclerosis: a complicated picture of autoimmunity. *Nat. Immunol.* **8,** 913–919
4. Dutta, R., and Trapp, B. D. (2007) Pathogenesis of axonal and neuronal damage in multiple sclerosis. *Neurology* **68,** S22–S31; discussion S43–S54
5. Sospedra, M., and Martin, R. (2005) Immunology of multiple sclerosis. *Annu. Rev. Immunol.* **23,** 683–747
6. Pettinelli, C. B., and McFarlin, D. E. (1981) Adoptive transfer of experimental allergic encephalomyelitis in SJL/J mice after *in vitro* activation of lymph node cells by myelin basic protein: requirement for Lyt 1+ 2- T lymphocytes. *J. Immunol.* **127,** 1420–1423
7. Zamvil, S. S., and Steinman, L. (1990) The T lymphocyte in experimental allergic encephalomyelitis. *Annu. Rev. Immunol.* **8,** 579–621
8. Huseby, E. S., Liggitt, D., Brabb, T., Schnabel, B., Ohlén, C., and Goverman, J. (2001) A pathogenic role for myelin-specific CD8(+) T cells in a model for multiple sclerosis. *J. Exp. Med.* **194,** 669–676
9. Archelos, J. J., Storch, M. K., and Hartung, H. P. (2000) The role of B cells and autoantibodies in multiple sclerosis. *Ann. Neurol.* **47,** 694–706
10. Genain, C. P., Cannella, B., Hauser, S. L., and Raine, C. S. (1999) Identification of autoantibodies associated with myelin damage in multiple sclerosis. *Nat. Med.* **5,** 170–175
11. Esiri, M. M. (1977) Immunoglobulin-containing cells in multiple-sclerosis plaques. *Lancet* **2,** 478
12. Sayed, B. A., Walker, M. E., and Brown, M. A. (2011) Cutting edge: mast cells regulate disease severity in a relapsing-remitting model of multiple sclerosis. *J. Immunol.* **186,** 3294–3298
13. Zappulla, J. P., Arock, M., Mars, L. T., and Liblau, R. S. (2002) Mast cells: new targets for multiple sclerosis therapy? *J. Neuroimmunol.* **131,** 5–20
14. Dijkstra, C. D., De Groot, C. J., and Huitinga, I. (1992) The role of macrophages in demyelination. *J. Neuroimmunol.* **40,** 183–188
15. Kang, Z., Altuntas, C. Z., Gulen, M. F., Liu, C., Giltiay, N., Qin, H., Liu, L., Qian, W., Ransohoff, R. M., Bergmann, C., Stohlman, S., Tuohy, V. K., and Li, X. (2010) Astrocyte-restricted ablation of interleukin-17-induced Act1-mediated signaling ameliorates autoimmune encephalomyelitis. *Immunity* **32,** 414–425
16. Heppner, F. L., Greter, M., Marino, D., Falsig, J., Raivich, G., Hövelmeyer, N., Waisman, A., Rülicke, T., Prinz, M., Priller, J., Becher, B., and Aguzzi, A. (2005) Experimental autoimmune encephalomyelitis repressed by microglial paralysis. *Nat. Med.* **11,** 146–152
17. Wang, Y., Kai, H., Chang, F., Shibata, K., Tahara-Hanaoka, S., Honda, S., Shibuya, A., and Shibuya, K. (2007) A critical role of LFA-1 in the development of Th17 cells and induction of experimental autoimmune encephalomyelytis. *Biochem. Biophys. Res. Commun.* **353,** 857–862
18. Bullard, D. C., Hu, X., Schoeb, T. R., Collins, R. G., Beaudet, A. L., and Barnum, S. R. (2007) Intercellular adhesion molecule-1 expression is required on multiple cell types for the development of experimental autoimmune encephalomyelitis. *J. Immunol.* **178,** 851–857
19. Zhang, G. X., Baker, C. M., Kolson, D. L., and Rostami, A. M. (2000) Chemokines and chemokine receptors in the pathogenesis of multiple sclerosis. *Mult. Scler.* **6,** 3–13
20. Tran, E. H., Prince, E. N., and Owens, T. (2000) IFN-γ shapes immune invasion of the central nervous system via regulation of chemokines. *J. Immunol.* **164,** 2759–2768
21. Hraba-Renevey, S., Türler, H., Kress, M., Salomon, C., and Weil, R. (1989) SV40-induced expression of mouse gene 24p3 involves a post-transcriptional mechanism. *Oncogene* **4,** 601–608
22. Liu, Q., and Nilsen-Hamilton, M. (1995) Identification of a new acute phase protein. *J. Biol. Chem.* **270,** 22565–22570

23. Cowland, J. B., and Borregaard, N. (1997) Molecular characterization and pattern of tissue expression of the gene for neutrophil gelatinase-associated lipocalin from humans. *Genomics* **45,** 17–23
24. Akerstrom, B., Flower, D. R., and Salier, J. P. (2000) Lipocalins: unity in diversity. *Biochim. Biophys. Acta* **1482,** 1–8
25. Flower, D. R. (1996) The lipocalin protein family: structure and function. *Biochem. J.* **318,** 1–14
26. Flower, D. R. (1994) The lipocalin protein family: a role in cell regulation. *FEBS Lett.* **354,** 7–11
27. Bauer, M., Eickhoff, J. C., Gould, M. N., Mundhenke, C., Maass, N., and Friedl, A. (2008) Neutrophil gelatinase-associated lipocalin (NGAL) is a predictor of poor prognosis in human primary breast cancer. *Breast Cancer Res. Treat.* **108,** 389–397
28. Devireddy, L. R., Gazin, C., Zhu, X., and Green, M. R. (2005) A cell-surface receptor for lipocalin 24p3 selectively mediates apoptosis and iron uptake. *Cell* **123,** 1293–1305
29. Tong, Z., Wu, X., Ovcharenko, D., Zhu, J., Chen, C. S., and Kehrer, J. P. (2005) Neutrophil gelatinase-associated lipocalin as a survival factor. *Biochem. J.* **391,** 441–448
30. Yang, J., Goetz, D., Li, J. Y., Wang, W., Mori, K., Setlik, D., Du, T., Erdjument-Bromage, H., Tempst, P., Strong, R., and Barasch, J. (2002) An iron delivery pathway mediated by a lipocalin. *Mol. Cell* **10,** 1045–1056
31. Nielsen, B. S., Borregaard, N., Bundgaard, J. R., Timshel, S., Sehested, M., and Kjeldsen, L. (1996) Induction of NGAL synthesis in epithelial cells of human colorectal neoplasia and inflammatory bowel diseases. *Gut.* **38,** 414–420
32. Nomura, I., Gao, B., Boguniewicz, M., Darst, M. A., Travers, J. B., and Leung, D. Y. (2003) Distinct patterns of gene expression in the skin lesions of atopic dermatitis and psoriasis: a gene microarray analysis. *J. Allergy Clin. Immunol.* **112,** 1195–1202
33. Katano, M., Okamoto, K., Arito, M., Kawakami, Y., Kurokawa, M. S., Suematsu, N., Shimada, S., Nakamura, H., Xiang, Y., Masuko, K., Nishioka, K., Yudoh, K., and Kato, T. (2009) Implication of granulocyte-macrophage colony-stimulating factor induced neutrophil gelatinase-associated lipocalin in pathogenesis of rheumatoid arthritis revealed by proteome analysis. *Arthritis Res. Ther.* **11,** R3
34. Javierre, B. M., Fernandez, A. F., Richter, J., Al-Shahrour, F., Martin-Subero, J. I., Rodriguez-Ubreva, J., Berdasco, M., Fraga, M. F., O'Hanlon, T. P., Rider, L. G., Jacinto, F. V., Lopez-Longo, F. J., Dopazo, J., Forn, M., Peinado, M. A., Carreño, L., Sawalha, A. H., Harley, J. B., Siebert, R., Esteller, M., Miller, F. W., and Ballestar, E. (2010) Changes in the pattern of DNA methylation associate with twin discordance in systemic lupus erythematosus. *Genome Res.* **20,** 170–179
35. Shen, F., Hu, Z., Goswami, J., and Gaffen, S. L. (2006) Identification of common transcriptional regulatory elements in interleukin-17 target genes. *J. Biol. Chem.* **281,** 24138–24148
36. Shen, F., Ruddy, M. J., Plamondon, P., and Gaffen, S. L. (2005) Cytokines link osteoblasts and inflammation: microarray analysis of interleukin-17- and TNF-α-induced genes in bone cells. *J. Leukoc. Biol.* **77,** 388–399
37. Choi, J., Lee, H. W., and Suk, K. (2011) Increased plasma levels of lipocalin 2 in mild cognitive impairment. *J. Neurol. Sci.* **305,** 28–33
38. Naudé, P. J., Nyakas, C., Eiden, L. E., Ait-Ali, D., van der Heide, R., Engelborghs, S., Luiten, P. G., De Deyn, P. P., den Boer, J. A., and Eisel, U. L. (2012) Lipocalin 2: novel component of proinflammatory signaling in Alzheimer's disease. *FASEB J.* **26,** 2811–2823
39. Tong, J., Huang, C., Bi, F., Wu, Q., Huang, B., Liu, X., Li, F., Zhou, H., and Xia, X. G. (2013) Expression of ALS-linked TDP-43 mutant in astrocytes causes non-cell-autonomous motor neuron death in rats. *EMBO J.* **32,** 1917–1926
40. Bi, F., Huang, C., Tong, J., Qiu, G., Huang, B., Wu, Q., Li, F., Xu, Z., Bowser, R., Xia, X. G., and Zhou, H. (2013) Reactive astrocytes secrete lcn2 to promote neuron death. *Proc. Natl. Acad. Sci. U.S.A.* **110,** 4069–4074
41. Lee, S., Park, J. Y., Lee, W. H., Kim, H., Park, H. C., Mori, K., and Suk, K. (2009) Lipocalin-2 is an autocrine mediator of reactive astrocytosis. *J. Neurosci.* **29,** 234–249
42. Lee, S., Kim, J. H., Kim, J. H., Seo, J. W., Han, H. S., Lee, W. H., Mori, K., Nakao, K., Barasch, J., and Suk, K. (2011) Lipocalin-2 is a chemokine inducer in the central nervous system: role of chemokine ligand 10 (CXCL10) in lipocalin-2-induced cell migration. *J. Biol. Chem.* **286,** 43855–43870
43. Jang, E., Lee, S., Kim, J. H., Kim, J. H., Seo, J. W., Lee, W. H., Mori, K., Nakao, K., and Suk, K. (2013) Secreted protein lipocalin-2 promotes microglial M1 polarization. *FASEB J.* **27,** 1176–1190
44. Ip, J. P., Noçon, A. L., Hofer, M. J., Lim, S. L., Müller, M., and Campbell, I. L. (2011) Lipocalin 2 in the central nervous system host response to systemic lipopolysaccharide administration. *J. Neuroinflammation* **8,** 124
45. Chia, W. J., Dawe, G. S., and Ong, W. Y. (2011) Expression and localization of the iron-siderophore binding protein lipocalin 2 in the normal rat brain and after kainate-induced excitotoxicity. *Neurochem. Int.* **59,** 591–599
46. Rathore, K. I., Berard, J. L., Redensek, A., Chierzi, S., Lopez-Vales, R., Santos, M., Akira, S., and David, S. (2011) Lipocalin 2 plays an immunomodulatory role and has detrimental effects after spinal cord injury. *J. Neurosci.* **31,** 13412–13419
47. Lee, S., Lee, W. H., Lee, M. S., Mori, K., and Suk, K. (2012) Regulation by lipocalin-2 of neuronal cell death, migration, and morphology. *J. Neurosci. Res.* **90,** 540–550
48. Mucha, M., Skrzypiec, A. E., Schiavon, E., Attwood, B. K., Kucerova, E., and Pawlak, R. (2011) Lipocalin-2 controls neuronal excitability and anxiety by regulating dendritic spine formation and maturation. *Proc. Natl. Acad. Sci. U.S.A.* **108,** 18436–18441
49. Nairz, M., Theurl, I., Schroll, A., Theurl, M., Fritsche, G., Lindner, E., Seifert, M., Crouch, M. L., Hantke, K., Akira, S., Fang, F. C., and Weiss, G. (2009) Absence of functional Hfe protects mice from invasive *Salmonella enterica* serovar *Typhimurium* infection via induction of lipocalin-2. *Blood* **114,** 3642–3651
50. Flo, T. H., Smith, K. D., Sato, S., Rodriguez, D. J., Holmes, M. A., Strong, R. K., Akira, S., and Aderem, A. (2004) Lipocalin 2 mediates an innate immune response to bacterial infection by sequestrating iron. *Nature* **432,** 917–921
51. Jiang, H. R., Al Rasebi, Z., Mensah-Brown, E., Shahin, A., Xu, D., Goodyear, C. S., Fukada, S. Y., Liu, F. T., Liew, F. Y., and Lukic, M. L. (2009) Galectin-3 deficiency reduces the severity of experimental autoimmune encephalomyelitis. *J. Immunol.* **182,** 1167–1173
52. Flügel, A., Berkowicz, T., Ritter, T., Labeur, M., Jenne, D. E., Li, Z., Ellwart, J. W., Willem, M., Lassmann, H., and Wekerle, H. (2001) Migratory activity and functional changes of green fluorescent effector cells before and during experimental autoimmune encephalomyelitis. *Immunity* **14,** 547–560
53. Zamanian, J. L., Xu, L., Foo, L. C., Nouri, N., Zhou, L., Giffard, R. G., and Barres, B. A. (2012) Genomic analysis of reactive astrogliosis. *J. Neurosci.* **32,** 6391–6410
54. Lin, Y., Roberts, T. J., Sriram, V., Cho, S., and Brutkiewicz, R. R. (2003) Myeloid marker expression on antiviral CD8+ T cells following an acute virus infection. *Eur. J. Immunol.* **33,** 2736–2743
55. Lee, S., Lee, J., Kim, S., Park, J. Y., Lee, W. H., Mori, K., Kim, S. H., Kim, I. K., and Suk, K. (2007) A dual role of lipocalin 2 in the apoptosis and deramification of activated microglia. *J. Immunol.* **179,** 3231–3241
56. Jeon, S., Jha, M. K., Ock, J., Seo, J., Jin, M., Cho, H., Lee, W. H., and Suk, K. (2013) Role of lipocalin-2-chemokine axis in the development of neuropathic pain following peripheral nerve injury. *J. Biol. Chem.* **288,** 24116–24127
57. Glass, C. K., Saijo, K., Winner, B., Marchetto, M. C., and Gage, F. H. (2010) Mechanisms underlying inflammation in neurodegeneration. *Cell* **140,** 918–934
58. Stromnes, I. M., Cerretti, L. M., Liggitt, D., Harris, R. A., and Goverman, J. M. (2008) Differential regulation of central nervous system autoimmunity by T(H)1 and T(H)17 cells. *Nat. Med.* **14,** 337–342
59. Cornet, A., Bettelli, E., Oukka, M., Cambouris, C., Avellana-Adalid, V., Kosmatopoulos, K., and Liblau, R. S. (2000) Role of astrocytes in antigen presentation and naive T-cell activation. *J. Neuroimmunol.* **106,** 69–77
60. Panek, R. B., Lee, Y. J., Itoh-Lindstrom, Y., Ting, J. P., and Benveniste, E. N. (1994) Characterization of astrocyte nuclear proteins involved in IFN-γ- and TNF-α-mediated class II MHC gene expression. *J. Immunol.* **153,** 4555–4564
61. Simpson, J., Rezaie, P., Newcombe, J., Cuzner, M. L., Male, D., and Woodroofe, M. N. (2000) Expression of the β-chemokine receptors CCR2, CCR3, and CCR5 in multiple sclerosis central nervous system tis-

sue. *J. Neuroimmunol.* **108,** 192–200
62. Van Der Voorn, P., Tekstra, J., Beelen, R. H., Tensen, C. P., Van Der Valk, P., and De Groot, C. J. (1999) Expression of MCP-1 by reactive astrocytes in demyelinating multiple sclerosis lesions. *Am. J. Pathol.* **154,** 45–51
63. Ransohoff, R. M., Hamilton, T. A., Tani, M., Stoler, M. H., Shick, H. E., Major, J. A., Estes, M. L., Thomas, D. M., and Tuohy, V. K. (1993) Astrocyte expression of mRNA encoding cytokines IP-10 and JE/MCP-1 in experimental autoimmune encephalomyelitis. *FASEB J.* **7,** 592–600
64. Gijbels, K., Masure, S., Carton, H., and Opdenakker, G. (1992) Gelatinase in the cerebrospinal fluid of patients with multiple sclerosis and other inflammatory neurological disorders. *J. Neuroimmunol.* **41,** 29–34
65. Gijbels, K., Galardy, R. E., and Steinman, L. (1994) Reversal of experimental autoimmune encephalomyelitis with a hydroxamate inhibitor of matrix metalloproteases. *J. Clin. Invest.* **94,** 2177–2182
66. Yan, L., Borregaard, N., Kjeldsen, L., and Moses, M. A. (2001) The high molecular weight urinary matrix metalloproteinase (MMP) activity is a complex of gelatinase B/MMP-9 and neutrophil gelatinase-associated lipocalin (NGAL). Modulation of MMP-9 activity by NGAL. *J. Biol. Chem.* **276,** 37258–37265
67. Tschesche, H., Zölzer, V., Triebel, S., and Bartsch, S. (2001) The human neutrophil lipocalin supports the allosteric activation of matrix metalloproteinases. *Eur. J. Biochem.* **268,** 1918–1928
68. Yong, V. W., Power, C., Forsyth, P., and Edwards, D. R. (2001) Metalloproteinases in biology and pathology of the nervous system. *Nat. Rev. Neurosci.* **2,** 502–511
69. Crocker, S. J., Whitmire, J. K., Frausto, R. F., Chertboonmuang, P., Soloway, P. D., Whitton, J. L., and Campbell, I. L. (2006) Persistent macrophage/microglial activation and myelin disruption after experimental autoimmune encephalomyelitis in tissue inhibitor of metalloproteinase-1-deficient mice. *Am. J. Pathol.* **169,** 2104–2116
70. Summers, C., Rankin, S. M., Condliffe, A. M., Singh, N., Peters, A. M., and Chilvers, E. R. (2010) Neutrophil kinetics in health and disease. *Trends Immunol.* **31,** 318–324
71. Puga, I., Cols, M., Barra, C. M., He, B., Cassis, L., Gentile, M., Comerma, L., Chorny, A., Shan, M., Xu, W., Magri, G., Knowles, D. M., Tam, W., Chiu, A., Bussel, J. B., Serrano, S., Lorente, J. A., Bellosillo, B., Lloreta, J., Juanpere, N., Alameda, F., Baró, T., de Heredia, C. D., Torán, N., Català, A., Torrebadell, M., Fortuny, C., Cusí, V., Carreras, C., Diaz, G. A., Blander, J. M., Farber, C. M., Silvestri, G., Cunningham-Rundles, C., Calvillo, M., Dufour, C., Notarangelo, L. D., Lougaris, V., Plebani, A., Casanova, J. L., Ganal, S. C., Diefenbach, A., Aróstegui, J. I., Juan, M., Yagüe, J., Mahlaoui, N., Donadieu, J., Chen, K., and Cerutti, A. (2012) B cell-helper neutrophils stimulate the diversification and production of immunoglobulin in the marginal zone of the spleen. *Nat. Immunol.* **13,** 170–180
72. Soehnlein, O. (2009) An elegant defense: how neutrophils shape the immune response. *Trends Immunol.* **30,** 511–512
73. van Gisbergen, K. P., Sanchez-Hernandez, M., Geijtenbeek, T. B., and van Kooyk, Y. (2005) Neutrophils mediate immune modulation of dendritic cells through glycosylation-dependent interactions between Mac-1 and DC-SIGN. *J. Exp. Med.* **201,** 1281–1292
74. Berard, J. L., Zarruk, J. G., Arbour, N., Prat, A., Yong, V. W., Jacques, F. H., Akira, S., and David, S. (2012) Lipocalin 2 is a novel immune mediator of experimental autoimmune encephalomyelitis pathogenesis and is modulated in multiple sclerosis. *Glia* **60,** 1145–1159
75. Marques, F., Mesquita, S. D., Sousa, J. C., Coppola, G., Gao, F., Geschwind, D. H., Columba-Cabezas, S., Aloisi, F., Degn, M., Cerqueira, J. J., Sousa, N., Correia-Neves, M., and Palha, J. A. (2012) Lipocalin 2 is present in the EAE brain and is modulated by natalizumab. *Front. Cell. Neurosci.* **6,** 33
76. Hawlisch, H., Wills-Karp, M., Karp, C. L., and Köhl, J. (2004) The anaphylatoxins bridge innate and adaptive immune responses in allergic asthma. *Mol. Immunol.* **41,** 123–131
77. Köhl, J. (2006) Self, non-self, and danger: a complementary view. *Adv. Exp. Med. Biol.* **586,** 71–94
78. Szalai, A. J., Hu, X., Adams, J. E., and Barnum, S. R. (2007) Complement in experimental autoimmune encephalomyelitis revisited: C3 is required for development of maximal disease. *Mol. Immunol.* **44,** 3132–3136
79. Nataf, S., Carroll, S. L., Wetsel, R. A., Szalai, A. J., and Barnum, S. R. (2000) Attenuation of experimental autoimmune demyelination in complement-deficient mice. *J. Immunol.* **165,** 5867–5873
80. Luchtefeld, M., Preuss, C., Rühle, F., Bogalle, E. P., Sietmann, A., Figura, S., Müller, W., Grote, K., Schieffer, B., and Stoll, M. (2011) Gp130-dependent release of acute phase proteins is linked to the activation of innate immune signaling pathways. *PLoS ONE* **6,** e19427
81. Korn, T., Mitsdoerffer, M., Croxford, A. L., Awasthi, A., Dardalhon, V. A., Galileos, G., Vollmar, P., Stritesky, G. L., Kaplan, M. H., Waisman, A., Kuchroo, V. K., and Oukka, M. (2008) IL-6 controls Th17 immunity *in vivo* by inhibiting the conversion of conventional T cells into Foxp3+ regulatory T cells. *Proc. Natl. Acad. Sci. U.S.A.* **105,** 18460–18465